ABSTRACT

Title of Document: PHYLOGENETIC RELATIONSHIP AMONG POLYMORPHIC OLIGOHYMENOPHOREAN CILIATES, WITH GENE EXPRESSION IN LIFE-HISTORY STAGES OF *MIAMIENSIS AVIDUS* (CILIOPHORA, OLIGOHYMENOPHOREA)

Glenn Frederick Gebler
Doctor of Philosophy, 2007

Directed By: Dr. Eugene B. Small
Department of Biology

The Class Oligohymenophorea is a monophyletic group possessing polymorphic taxa. Thus far, relationships within subclasses of oligohymenophorean ciliates and between polymorphic taxa within families are not well resolved. Here, nuclear small subunit rRNA (SSU rRNA) gene sequences from 63 representative taxa, including several polymorphic species, were used to construct phylogenies and test monophyly of the subclass Scuticociliatia and of the polymorphic taxa within the Oligohymenophorea. In addition, suppression subtraction hybridization (SSH) was used to test the hypothesis that genes are differentially expressed during microstome-to-macrostome and tomite-to-microstome transformation in the polymorphic scuticociliate *Miamiensis avidus*. Phylogenetic analyses confirmed monophyly of the subclasses Peritrichia and Hymenostomatia. The monophyletic scuticociliates

encompassed most, but not all, taxa included in this study. The conditional acceptance of the hypothesis supporting monophyly of the Scuticociliatia was due to the ambiguous placement of three taxa, the apostome *Anoplophrya marylandensis*, the scuticociliate *Dexitrichides pangi*, and the peniculine *Urocentrum turbo*. The polymorphic trait most likely arose on at least four, and perhaps on as many as six, separate occasions within the oligohymenophorean ciliates. Several genes previously implicated in morphogenetic processes in eukaryotes were upregulated during microstome-to-macrostome transformation in *M. avidus*. Those genes were, elongation factor-1 alpha (*Ef-1*α), Constans, Constans-like TOC1 (CCT) transcription factor, a disulfide isomerase, heat shock protein 70, step II splicing factor (*Slu7*), U1 zinc finger protein, and WD40-16 repeat protein. A similar analysis for *M. avidus* undergoing tomite-to-microstome transformation identified genes previously linked to transformation processes in other protists: two cysteine protease genes lacking formal description (papain-family and *XCP1* cysteine protease), two described cysteine protease genes, cathepsin B and cathepsin L, and one cysteine protease inhibitor (cystatin-1) gene. The roles of candidate genes for regulation of *M. avidus* life-history stages (*Ef-1*α for microstome-to-macrostome transformation; cathepsin B and cathepsin L for tomite-to-microstome transformation) were examined using pharmacological inhibition experiments. Drug treatments significantly reduced transformation of *M. avidus* microstomes into macrostomes within 6 h and prevented tomite-to-microstome transformation after 2.5 h. Results indicated that genes specifically linked to oral transformation in *M. avidus* are differentially expressed during microstome-macrostome and tomite-microstome transformation. Thus, this

study used molecular techniques to understand the evolutionary history and development of polymorphism within the Oligohymenophorean ciliates.

PHYLOGENETIC RELATIONSHIP AMONG POLYMORPHIC OLIGOHYMENOPHOREAN CILIATES, WITH GENE EXPRESSION IN LIFE-HISTORY STAGES OF *MIAMIENSIS AVIDUS* (CILIOPHORA, OLIGOHYMENOPHOREA)

By

Glenn Frederick Gebler

Dissertation submitted to the Faculty of the Graduate School of the
University of Maryland, College Park, in partial fulfillment
of the requirements for the degree of
Doctor of Philosophy
2007

Advisory Committee:
Professor Eugene B. Small, Chair
Professor William R. Jeffery
Professor Charles Mitter
Professor Alexandra E. Bely
Professor William J. Higgins

Dedication

To the life and memory of Dr. Roderick A. Scofield, an accomplished research scientist, an extraordinary human being, and a life-long friend.

Acknowledgements

I wish to thank Dr. Eugene B. Small, my primary advisor, who introduced me to the world of biology from the perspective of a ciliate. Gene was more than patient with my scientific questions and explorations. He guided me through my graduate experience and encouraged outreach and collaboration with others.

I am indebted to both Dr. William R. Jeffery and Dr. D. Wayne Coats. Both provided supervision and guidance through the completion of this work at crucial moments of its progress. Both contributed to my evolution as a scientist. I am grateful for their generosity, their time, and supervision. This work possibly would not have been completed without their assistance.

I am grateful for the participation of all of my committee members who improved the quality of my education, offered valuable insight, and supported the direction of this project. I would like to acknowledge Dr. Charles Mitter who introduced me to, and provided valuable education concerning phylogenetic theory and its applications.

I am also indebted to Dr. Allen Strickler, formerly of Dr. Jeffery's lab and a friend who spent numerous hours discussing subtraction suppression hybridization (SSH) techniques and improved my understanding of many molecular techniques. He never tired of my questions and I am grateful for his time.

I am equally indebted to Dr. Ken Karol, formerly of Dr. Charles Delwiche's lab for his friendship and his tutelage improving my understanding of molecular evolution, models of sequence evolution, phylogenetics, and life in general.

I am grateful for the love and support of my parents and my sister. In a multitude of ways, they helped me endure through challenging times. I am blessed to share my life with the three of them. I am also thankful for the love and support of Ms. Christi Lockard, my partner. In a lot of ways, this accomplishment is as much hers as it is mine. She has been patient with me through the critical evolution of this project and its completion. I look forward to our lives beyond graduate school.

I am grateful for the friendships with Dr. David Booth, Dr. Simon Gelman, Dr. Michael Dandenault, Mr. Ernie Hixon, and Ms. Laura Craig. I wish to thank all of the graduate students in the labs of Dr. William Jeffery, Dr. Eric Haag, Dr. Charles Delwiche, Dr. Kerry Shaw, and Dr. Matt Hare for their assistance and engaging discussions.

Lastly, I am thankful for the guidance and counsel of Ms. Lois Reid and the rest of the supportive staff in the business and the front offices. I thank you for helping me stay on track and up-to-date concerning deadlines and meetings. I am additionally grateful to the Department of Biology for its financial support provided in the Chesapeake Bay Fund awards that I received summer 2001-through-2006.

Table of Contents

List of Tables

List of Figures

Chapter 1: Overview of Oligohymenophorean Systematics and Polymorphism

Oligohymenophorean Systematics and Related Research Goals

Phylogenetic placement of the Ciliophora within the Kingdom Protista has undergone many revisions since Butschli (1880) first grouped the Protozoa into the Sarcodina (amoeboid organisms), the Sporozoa (parasitic organisms), the Masitigophora (flagellated organisms) and the Infusoria (ciliated organisms). Members of the Ciliophora are unified by several synapomorphies, including nuclear dimorphism represented by transcriptionally-inactive germinative micronuclei and transcriptionally-active macronuclei, presence of locomotory cilia organized as longitudinal rows over the somatic surface, kinetosomes (= basal bodies) and associated network of cytoskeletal fibers anchoring the cilia, ciliated oral structures that are replicated during cell division by a process known as stomatogenesis, and sexuality with nuclear recombination (Curry and Butler, 1982) These attributes have long been used to support the notion that the ciliates represent a monophyletic group of protists (Corliss, 1972; Corliss, 1979; Fauré-Fremiet, 1950; Lynn and Small, 2000; Small and Lynn, 1985).

With the development of new staining methods (e.g., Chatton-Lwoff and Protargol silver-staining) and the introduction of electron microscopy, came enhanced

recognition of protistan diversity. Recent ciliate classification schemes categorized taxa by similarities in oral structures, somatic ciliation, and somatic infraciliature (Corliss, 1974; Corliss, 1979; Lynn and Small, 2000; Small and Lynn, 1985). Diverse patterns of somatic and oral ciliature were used to place taxa in seven ciliate classes (Lynn and Small, 2000; and Small and Lynn, 1985). Somatic ciliation is composed of discrete ciliary units called kinetids, having one (monokinetid), two (dikinetid), or many (polykinetid) kinetosomes (Fauré-Fremiet, 1956; Lynn and Small, 2000; Small and Lynn, 1985; and Small, 1967). Kinetosomes of mono-, di-, and polykinetids may or may not bear cilia. Somatic kinetids are arranged in longitudinal rows in most species, but some ciliates have few to many somatic kinetids distributed in varied patterns on the ventral and/or dorsal surface. Ciliate oral structures are equally diverse and are accompanied by varied specializations in microtubule-based cytostomal elements (Corliss, 1974; Corliss, 1979; Lynn and Small, 2000; Small and Lynn, 1985). Many different systems of classification have been proposed for the Ciliophora using morphological characteristics (Adl et al., 2005; Corliss, 1974; Corlisss 1979, de Puytorac et. al., 1984; Jankowski, 1967, 1985; Lynn and Small, 2000; Small and Lynn, 1985), with most reflecting intuitive interpretation of ancestral morphological traits. However, more recent schemes have considered relationships revealed by molecular markers (Schmidt et al., 2007; Snoeyenbos et al., 2004; Stechmann et al., 1998; Wright et al., 1997).

Early molecular phylogenies for the Ciliophora utilized data for a few taxa from each of the seven ciliate classes (Lynn and Small, 2000; Small and Lynn, 1985). Those studies were limited by the small number of sequences available for ciliates, as well as limited computational power for analyzing large data sets. More recently, large data sets have been used to address unresolved questions about the evolution of some, but not all groups within the Ciliophora. For example, SSU (SSU) rRNA gene sequences were used to test hypotheses of monophyly of the ciliate classes Heterotrichea, Phyllopharyngea, Prostomatea, Colpoda, Nassophorea, and Litostomatea (Schmidt et al., 2007; Snoeyenbos et al., 2004; Stechmann et al., 1998; Wright et al., 1997). Likewise, Schmidt et al. (2007) used nuclear SSU rRNA gene sequences to propose an evolutionary process that gave rise to the eighteen cirri (fused cilia of somatic polykineties) on the ventral surface of spirotrich ciliates. Although molecular data has been used to confirm the relationship of these ciliate groups, the molecular phylogeny of the remaining class of ciliates, the Oligohymenophorea, is incomplete. Relationships within subclasses of oligohymenophorean ciliates and between polymorphic taxa within oligohymenophorean subclasses are not well-resolved.

Historically, morphological characters such as the orientation of several cortical fibers and microtubular structures associated with the kinetosome (e.g., kinetodesmal fiber, post-ciliary microtubules, transverse microtubular ribbons) were used to establish oigohymenophorean classification schemes. Ciliates in the

Hymenostomatia, Scuticociliatia, Peniculia, and Peritrichia were also unified by species having similar oral structures that included feeding membranelles and a ventral groove leading to a cytostome-cytopharynx (Corliss, 1979; Lynn and Small, 2000; Small and Lynn, 1985). While these general synapomorphies have been used to place ciliates in the Olighymenophorea, some members lack one or more morphological characteristics used to establish monophyly of the class. For example, the Astomatia have characteristic oligohymenophorean fibers and microtubular structures associated with their somatic ciliary bases, yet they lack oral structures (Corliss, 1979). By contrast, the Peritrichia lack somatic ciliature (except at their telotroch band), but have characteristic oligohymenophorean oral kineties (Corliss, 1979; Lynn and Small, 2000; Small and Lynn, 1985).

Many Oligohymenophorean species have complex life histories including oral replacement in response to prey abundance and quality (Gomez-Saladin and Small 1993a-c). Oral replacement is one type of polymorphism within the Oligohymenophorea and requires restructuring subcortical architecture associated with somatic and oral kineties. Most polymorphic hymenostomes and scuticociliates have morphologically distinct feeding stages including a bacteriovorous microstome, a predatory macrostome, and, in some instances, a non-feeding, fast swimming tomite (Corliss, 1972; Gomez-Saladin 1993a-c; Hoffman, 1975; Moewus, 1962; Ramsey et al., 1985a-b; Savoie, 1962; Thompson, 1966). Microstomes and macrostomes are also known for *Tetrahymena vorax* and *Tetrahymena paravorax*, but those species appear

to lack tomites (Corliss, 1972; and Williams et al. 1992). By contrast, microstomes and tomites, but not macrostomes have been reported for *Glauconema bermudiense* (Small et al., 1986).

Current morphological analyses place the polymorphic scuticociliates, *Miamiensis avidus* Strain Ma/2, *Glauconema bermudiense*, *Potomacus pottsi*, and *Urocryptum tortum* within the family Parauronematidae along with several non-polymorphic taxa (Gomez-Saladin and Small, 1993a-c; Moewus, 1962; Perez-Uz, 2001; Ramsey et al., 1981; Ramsey et al., 1985; Small, 1986; Thompson, 1966). *Tetrahymena paravorax*, *Tetrahymena vorax* Strain V_2, and *Tetrahymena patula*, are designated to the family Tetrahymenidae, which also includes several non-polymorphic tetrahymenines (Buhse, 1967; Keenan, 1973; Nijine, 1972; Nanney, 1976; Williams 1961). The parasitic hymenostomes *Ichthyophthirius multifillis* and *Ophryoglena catenula* are assigned to the exclusively polymorphic Ichthyophthiridae and its sister family the Ophryoglenidae, respectively (Hoffman, 1975 and Savoie, 1962).

Recent studies have used molecular data to established monophyly of the oligohymenophorean subclasses Hymenostomatia (Struder-Kypke, 2001), Peritrichia (Miao et al., 2004; Struder-Kupke et al., 2000; Utz and Eizirik, 2007), and the Peniculia (Struder-Kypke, 2000). Monophyly of the Scuticociliatia, Astomatia, and Apostomatia, however, have yet to be established using molecular sequences. At

present, too few sequences are available to test monophyly of the astomes, and no sequences are available for apostomes. While SSU rRNA gene sequences are available for a relatively large number of scuticociliate species, robust phylogenetic analyses of the group are lacking. Further, while monophyly has been established for three of the subclasses, molecular studies have not provided more detailed consideration of evolutionary patterns of polymorphic and non-polymorphic Oligohymenophorea. Thus, goals of this study included the use of SSU rRNA sequences to (1) test monophyly of the Scuticociliatia, (2) explore phylogenetic relationships among oligohymenophorean families, and (3) assess evolutionary patterns for polymorphic ciliates currently placed in the Hymenostomatia and Scuticociliatia.

Polymorphism of Miamiensis avidus Strain Ma/2 and Related Research Goals

The tripartite life-history of the polymorphic scuticociliate *Miamiensis avidus* Strain Ma/2 (Fig. 1-1) and the external cues that induce transformation from one life-history stage to another have been considered in detail by Gomez-Saladin and Small (1993a-c). In logarithmic growth, the predominant morphotype is the bactivorous microstome. Microstomes are pyriforme cells of medium size, possessing bipolar somatic kineties. The oral region is pre-equatorial, measuring ~1/3 of total cell length. Oral ciliature consists of three small polykineties, designated anterior to posterior as OPk 1, 2, and 3, and a dikinety that is separated into three segments designated

anterior to posterior as ODk A, B, and C. The cytostome is positioned mid-ventrally or posterior-ventrally and leads to a cytopharynx lacking a preparatory vacuole. The oral cilia are used to sweep bacterial prey into small food vacuoles that are typically numerous in the cytoplasm. While microsomes are bacteriovorous, they can be cultured in axenic, nutrient rich media.

When ciliate prey (e.g., *Paranophrys* sp.) are abundant, microstomes of *M. avidus* transform into predatory macrostomes (Gomez-Saladin and Small, 1993a-c). Fully differentiated macrostomes are large pyriforme cells with bipolar kineties and an oral area extending ~ 2/3 of total cell length. The oral polykineties of macrostomes are slightly larger than those of microstomes, but the oral dikinetids are much longer and the cytostome leads to a large preparatory vacuole capable of quickly enclosing small cilate prey. In axenic culture, high densities of microstomes or tomites (see below) can induce macrostome transformation. Microstomes transform into macrostomes by a process known as oral replacement. During oral replacement, microstome oral structure are dedifferentiated, leading to the formation of an anarchic field of kinetosome that serves as the anlage for in situ development of macrostome oral sructures. Buhse (1967) and Gomez-Saladin and Small (1993a) showed that microstome-to-macrostome transformation in *Tetrahymena vorax* and *Miamiensis avidus* respectively, is induced by washing microstomes into prey conditioned medium. In the case of *T. vorax*, the active compound in prey-conditioned medium that induces macrostome transformation is a peptide named stomatin by Buhse (1967).

When ciliate prey are depleted, microstomes transform into tomites by a process known as tomitogenesis (Gomez-Saladin and Small 1993a). During tomitogenesis, a process that takes ~ 6 h, microstomes divide twice, simultaneously undergoing oral reduction to produce small daughter cells that have reduced or incomplete oral ciliature. Tomites have bipolar kineties and are small, slender and rapidly swimming cells. They are viewed as an adaptive strategy to avoid starvation, representing a dispersal stage that transforms back into to microstomes when sufficiently high densities of bacterial prey are encountered. Returning tomites to nutrient media formulated with full strength sea water induces tomites to transformation back into microstome, a process that also requires ~ 6 h.

While prior studies have characterized environmental cues and morphogentic processes associated with life-history transformations in *M. avidus* and other polymorphic Oligohymenophorea, nothing is known about genes involved in these radical morphological transitions. Thus, a goal of this study was to use molecular techniques (1) to test the hypothesis that up-regulated genes initiate microstome-to-macrostome and tomite-to-microstome transformation in *M. avidus* and (2) to assess the potential role of up-regulated genes in transformation events using pharmacological inhibition experiments.

Figure 1-1. Life-history stages of *Miamiensis avidus* Strain Ma/2 adapted from Gomez-Saladin and Small (1993a). (a) microstome with many food vacuoles to digest bacteria prey, (b) macrostome with conspicuous ODks and cyotpharyngeal pouch to digest ciliate prey, (c) tomite with reduced oral structures and an empty food vacuole. ODkA, ODkB, and ODkC = oral dikinetid segments A, B, and C, respectively. OPk1, OPk2, and OPk3 = oral polykinetid segments 1, 2, and 3, respectively. CP = cytopharyngeal pouch. FV = food vacuole.

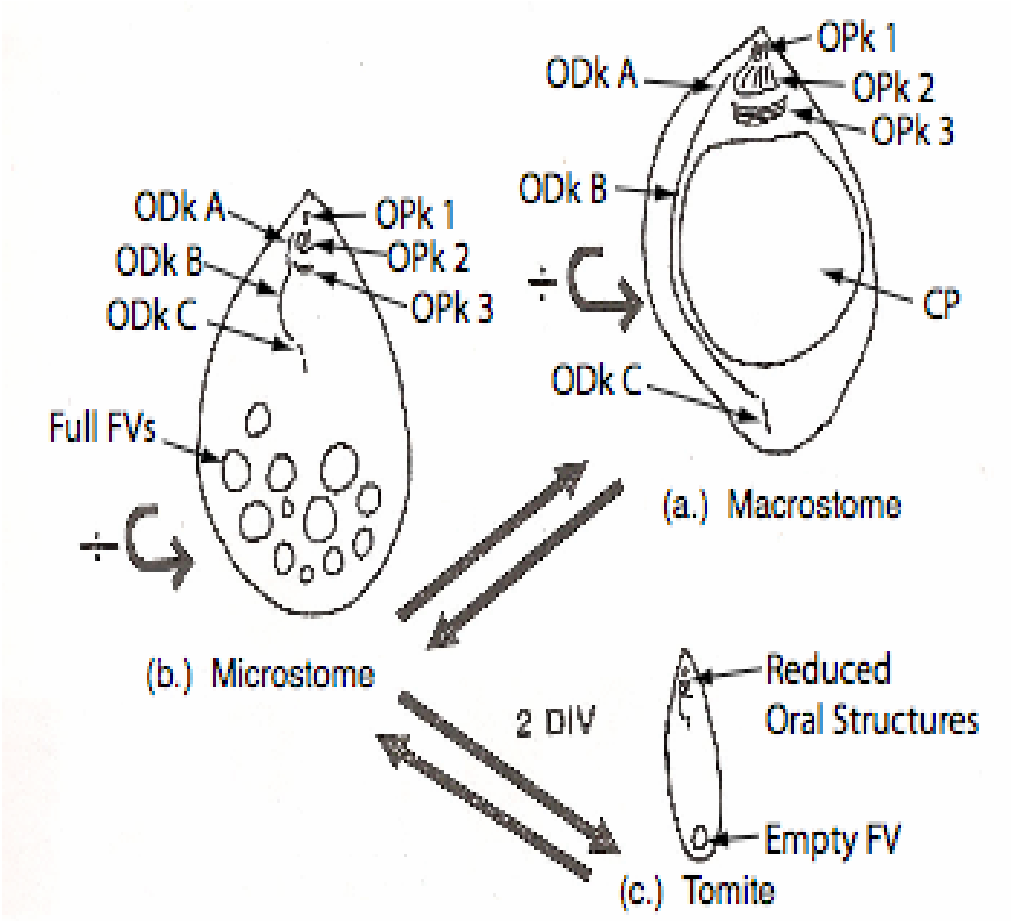
OPk 1
ODk A
OPk 2
OPk 3
ODk B
CP
ODk C
(a.) Macrostome
ODk A
OPk 1
ODk B
OPk 2
ODk C
OPk 3
Full FVs
(b.) Microstome
2 DIV
Reduced
Oral Structures
Empty FV
(c.) Tomite

Chapter 2: Phylogenetic Relationships Among Oligohymenophorean Ciliates Based on Small Subunit rRNA Gene Sequences, with Special Emphasis on Polymorphic Taxa.

Abstract

The Class Oligohymenophorea is a monophyletic group possessing many polymorphic taxa. Thus far, relationships within subclasses of oligohymenophorean ciliates and between polymorphic taxa within families are not well resolved. Here, nuclear small subunit rRNA gene sequences from 63 representative Oligohymenophorea taxa, including several polymorphic species, were used to construct a phylogeny for the Oligohymenophorea and to test monophyly of the subclass Scuticociliatia. The analyses confirmed monophyly of the subclasses Peritrichia and Hymenostomatia, but not the Scuticociliatia. The monophyly for the Scuticociliatia was accepted due largely to the exclusion of three taxa, the apostome *Anoplophrya marylandensis*, the scuticociliate *Dexitrichides pangi*, and the peniculine *Urocentrum turbo*. Additionally, a maximum parsimony tree was used to create a phylogenetic trace of the polymorphic character. That trace was used to determine the number of origins and losses of the polymorphic character within the Oligohymenophorea. The polymorphic scuticociliates clustered within the Parauronematidae along with non-polymorphic taxa. Similarly, the polymorphic Tetrahymenidae and Ophryiogenidae clustered with non-polymorphic taxa, but were

separated on different branches. The number of origins for the polymorphic trait was unambiguous in the Hymenostomatia, occurring on three separate occasions. The number of origins within the Scuticociliatia, however, was ambiguous, having arisen on as many as three occasions with up to two losses. Thus, the polymorphic trait arose on at least four, and perhaps on as many as six, separate occasions within the oligohymenophorean ciliates.

Introduction

Protistan systematics has been revised extensively since Butschlií's original one-phylum/four-class classification of the Protozoa (1889). Many of the changes in classification have resulted from technological advancements that permitted resolution of new characters distinctive of taxa. With improved resolution of distinct characters, came new insights concerning phylogenetic relationships among the protists. For example, enhanced imaging of living specimens led to the ciliates being raised to Phylum status in classification schemes of the mid-20th Century (Corliss, 1968; Honigberg, 1964). Further refinement of ciliate classification evolved through the introduction of silver-staining techniques and electron microscopy. Those approaches revealed variation in the orientation of cortical structures associated with ciliary bases (e.g., kinetodesmal fiber, post-ciliary microtubules, transverse microtubular ribbons), prompting Small & Lynn (1985) to recognize seven distinct classes within the Ciliophora (see Lynn & Small, 2000 for recent revisions). Most recently, the ability to develop gene sequences has proven valuable by furnishing robust data sets for testing phylogenies based on morphological characters. In some instances, molecular approaches have confirmed accepted ciliate classification schemes, but have on other occasions indicated polyphyletic and paraphyletic taxa requiring revision (Lynn and Small, 2000; Sogin, 1986; Spangler; 1985; Elwood, 1985).

The ciliate Class Oligohymenophorea was first proposed by de Puytorac (1974) and further refined by Corliss (1979) to include the subclasses Hymenostomatia, Scuticociliatia, Peniculia, and Peritrichia. The subclasses were unified by species having distinct oral cilia forming membranelles and a ventral groove leading to a cytostome-cytopharynx (Corliss, 1979). Later, Small and Lynn (1985) used ultrastructural features of the kinetome (i.e., fibers and microtubules associated with ciliary bases) to support inclusion of the astomes and apostomes as separate subclasses within Oligohymenophorea. Subsequently, molecular data confirmed placement of the monophyletic Hymenostomatia (Struder-Kypke, 2001), monophyletic Peritrichia (Utz and Eizirik, 2007; Wei Miao et al., 2004) and monophyletic Peniculia (Struder-Kypke, 2000) within the Class Oligohymenophorea. Monophyly of the three remaining subclasses (Scuticociliatia, Astomatia, and Apostomatia) has yet to be confirmed using molecular data.

Oligohymenophorean taxa incorporate several polymorphic strategies that contribute to their survival and distribution. These strategies include distinct life-history stages associated with feeding behavior [(bacterivory, predation, cannibalism) (Buchmann, 1999; Buhse, 1967; Gomez-Saladin and Small, 1993a-c)], parasitism (Bradbury, 1989; Bradbury, 2005; Corliss, 1972; Egerter 1986), encystment (Gabe and De Bault, 1973; McArdle et al. 1980; Perez-Uz, 2001), and dispersal (Clamp and Coats, 2000; Corliss, 1979; Miao, 2004). Polymorphism within the Oligohymenophorea includes the ability to restructure ciliature and subcortical

architecture associated with somatic and oral structures [(e.g., oral replacement in the tetrahymenines and scuticociliates) (Buhse, 1967; Gomez-Saladin, 1993a-c; Jung et al. 2007; Williams, 1961)]. In some instances, oligohymenophorean species incorporate several morphologically distinct stages within their life-history, each specialized for survival under different nutritional conditions (Fenchel, 1987). The capacity to rapidly switch morphotypes to contend with changing environments may provide an evolutionary, as well as survival advantage over monomorphic taxa.

Several species within the Hymenostomatia and Scuticociliatia exhibit multiple life-history stages adapted to different nutritional conditions. For example, the life-history of the polymorphic scuticociliate *Miamiensis avidus* includes microstomes, macrostomes, and tomites (Buhse, 1967; Gomez-Saladin, 1993a-c; Jung et al. 2007; Williams, 1961). Mircostomes are typically medium-sized, pyriforme-shape cells that have small mouths equipped with oral membranelles for feeding on bacteria. Microstomes can transform into macrostomes or tomites depending on availability of prey. Transition from microstomes to macrostomes involves oral replacement and is stimulated by low bacterial numbers and an abundance of ciliate prey. Oral replacement during macrostome formation encompasses reabsorption of the parental oral apparatus followed by *in situ* formation new, enlarged oral structures. These structures include elaborate oral membranelles and a large cytostome leading to a cytopharyngeal pouch capable of enclosing small to medium-sized ciliate prey. Transformation from microstomes to tomites also involves oral reduction and is

stimulated by low bacterial numbers and absence of ciliate prey. Oral reduction during tomite formation involves reabsorption of the parental oral ciliature. As a consequence, tomites are unable to feed and represent a small fast swimming dispersal stage. Similar life-histories incorporating oral replacements have also been reported for species of *Tetrahymena* and related genera (Buhse, 1967; and Williams, 1961).

Nine species of oligohymenophorean ciliates are known to have polymorphic life-histories involving oral replacement. Four of these, *Miamiensis avidus* Strain Ma/2 (Gomez-Saladin, 1993a-c, and Moewus, 1962), *Glauconema bermudiense* (Small, 1986), *Potomacus pottsi* (Ramsey, 1981; Ramsey, 1980; Thompson, 1966), and *Urocryptum tortum* (Perez-Uz, 2001) belong to the Scuticociliatia, while the remaining five *Tetrahymena paravorax* (Nijine, 1972; and Nanney, 1967), *Tetrahymena vorax* Strain V_2 (Buhse, 1967), *Tetrahymena patula* (Keenan, 1973; and Williams 1961), *Ichthyophthirius multifiliis* (Hoffman, 1975) and *Ophryoglena catenula* (Savoie, 1962) are members of the Hymenostomatia. Under the classification scheme of Lynn and Small (2000), the four polymorphic scuticociliates are assigned to the family Parauronematidae, which also includes several monomorphic species. Of the five polymorphic hymenostomes, one is assigned to the family Ichthyophthiriidae, one to the family Ophryoglenidae, and three to the family Tetrahymeniidae, which also includes monomorphic taxa. Thus far, molecular data are unavailable for evaluating the placement of polymorphic taxa within the two subclasses, or for testing relationships between polymorphic and non-polymorphic

taxa grouped within each family.

Here, I use nuclear small subunit rRNA gene sequences from 63 representative Oliohymenophorea taxa, including several polymorphic species, to construct a phylogeny for the Oligohymenophorea. The goals in constructing the phylogeny were to test for monophyly of the Scuticociliatia and to evaluate the validity of current familial assignment of polymorphic taxa within the scuticociliates and hymenostomes. Lastly, a character trace was conducted to assess the number of origins and deletions of the polymorphic trait within the class Oligohymenophorea.

Materials and Methods

Ciliate Cultures

Clonal cultures of the three polymorphic marine scuticociliates (*Miamiensis avidus* Strain Ma/2, *Potomacus pottsi*, and *Glauconema bermudiense*), three freshwater polymorphic hymenostomes (*Tetrahymena paravorax*, *Tetrahymena patula*, and *Tetrahymena vorax*), and nine non-polymorphic marine scuticociliates (Table 2-1) were obtained from the ATCC (American Type Culture Center, Manassas, VA). The marine species were grown in a trypticase peptone/protease peptone based medium (MA1651, ATCC) adjusted to 35 ppt salinity. The freshwater species were grown in nutrient protease peptone based media (MA357, ATCC, Manassas, VA). All cultures were maintained as 200-ml volumes in sterile 1-L flasks and incubated at 25 °C in the dark. To assure that cultures remained axenic, an aliquot was removed weekly from each culture and plated on nutrient agar (Fisher Scientific, Pittsburgh, PA, USA #S71613). Agar plates were incubated at 37 °C to for two days to allow growth and detection of possible bacterial contaminants. Subcultures that showed bacterial contamination were discarded.

DNA Extraction and Sequencing

Whole genome DNA was extracted from each cultured species. Additionally, lyophilized *Philasterides dicentrarchi* whole genome DNA was provided by Dr. Manuel Sanmartin Duran. For DNA extraction, 1-ml aliquots of cultured organisms (1×10^4 cells per aliquot) were harvested by light-centrifugation (200X g) in an Eppendorf 5414 centrifuge (Eppendorf, New York, New York, USA) and washed in 1X Phosphate Buffer Saline [(PBS), pH 7.0)] for freshwater species and 15X PBS (pH 7.0) for marine species. DNA was extracted from PBS-washed cells using Qiagen DNeasy Blood and Tissue Kit© (Qiagen, Valencia, CA, USA) following manufacture's recommendations, except that proteinase K incubation at 56 °C was for 3 hours instead of the recommended 10 minutes. All genomic DNA was stored at -20 °C in a frost-free freezer compartment of a refrigerator (General Electric Profile Energy Star, Fairfield, CT, USA) until amplified by polymerase chain reaction (PCR).

Small Subunit (SSU) rRNA genes of ciliate DNA were amplified by PCR performed in a Perkin Elmer GeneAmp 2400 thermocycler (PE Applied Biosystems, Foster City, CA, USA). Universal nuclear SSU rRNA primers, 5'Medlin Forward [5'-AACCTGGTTGAT CCTGCCAGT-3'] and 3'Medlin Reverse [5'-TGATCC TTCTGCAGGTT CACCTAC –3'] (Medlin et al., 1988), were used for DNA amplification. PCR reactions were in 100-µl volumes of 1X PCR Buffer (Qiagen,

Valencia, CA, USA), 0.025 U/µl Qiagen HotStarTaq DNA Polymerase, 2.5 mM $MgCl_2$, 0.5 µM forward and reverse primer, 200 µM of each dNTP, and approximately 200pg/µl template DNA. The thermocycler program was initiated with a heat activation step at 95 °C for 15 minutes, followed by 35 cycles of denaturing at 94 °C for 30 seconds, annealing at 68 °C for 1 minute, and final extension at 72 °C for 1.5 minutes. After the last cycle, a final extension step was set at 72 °C for 10 minutes. PCR products were purified by gel electrophoresis on 1% Agarose gel using QIAquick Gel Extraction Kit (Qiagen, Valencia, CA, USA, #1908).

SSU rRNA sequencing reactions were carried out in forward and reverse directions using ABI PRISM® BigDye® Terminator Cycle Sequencing Kit v3.1, according to the manufacturer's protocol, with resulting products resolved using an ABI-PRISM 377 DNA sequencer (PE Applied Biosystems, Foster City, CA, USA). The forward and reverse external primers of Medlin et al., (1988; see above) and four internal primers of Elwood et al., (1985) [C184 (5'-ACGAGCTTTTTAACTGCA-3'), N184 (5'-TGCAGTT AAAAAGCTCGT-3"), N181 (5'-AATTTGACTCAACA CGGG-3'), and C181 (5'-CCCGTGTTGA GTCAAATT-3'] were used to obtain complete SSU rRNA sequences. Sequence chromatograms were edited and assembled into a single alignment using the sequence analysis programs Jellyfish® (Field Scientific LLC, Lewisburg, PA, USA) and Geneious® (Drummond et al., 2006). Edited sequences were exported in NEXUS format for phylogenetic analysis.

Phylogenetic Analyses

Phylogenetic analyses were conducted using SSU rRNA sequences for 64 ciliate species (Table 2-2), of which 15 were determined as above and 49 were obtained from GenBank/NCBI. Sequences were selected from GenBank to ensure complete coverage of polymorphic Oligohymenophorea (2 additional species) and to include all available data for the subclasses Scuticociliatia (22 additional non-polymorphic species) and Astomatia (1 species). For the three remaining oligohymenophorean subclasses (Peritrichia, Peniculia, and Hymenostomatia), sequences of 7-10 species were chosen from Genbank to provide full representation of genera for which data were available. For all analyses, the species *Loxodes striatus*, a member from the Class Karyorelictea (NCBI accession number U24248), was selected as the outgroup taxon.

The 64 ciliate SSU rRNA sequences were globally aligned using Clustal X employing stringent gap penalties (0.01) followed by manual alignment using MacClade v4.05 (Thompson et al., 1997, Maddison, D. and Maddison, W., 1989). A hypervariable region (total of 42 base pairs in length) detected during alignment was excluded from the dataset, resulting in a final length of 1762 aligned base pairs for use in phylogenetic analyses.

Five separate phylogenetic analyses were used to assess relationships among the 64 ciliate species. Three of the analyses were based on maximum likelihood [Bayesian inference (BI), maximum likelihood (ML-PAUP), and Genetic Algorithm for Rapid Likelihood Inference (GARLI)], one was maximum parsimony, and one was a minimum evolution distance method. The three types of analyses were chosen to test hypotheses concerning differing models of sequence evolution, while the three maximum likelihood methods used different algorithms and assumptions for generating trees.

For Bayesian analysis, MrModeltest v2.2 (Nylander 2004, Dept. Systematic Zoology, EBC, Uppsala University, Sweden) indicated that the General Time Reversable+Invariant+Gamma (GTR+I+Γ) model best fit the data. Output estimates from the GTR+I+Γ model were thus incorporated into MrBayes 3.1.2 (Huelsenbeck and Ronquist, 2001 and Ronquist and Huelsenbeck, 2003) to generate trees from the SSU rRNA sequences. The “Metropolis-coupled Markov chain Monte Carlo” (MCMCMC) was chosen as the tree searching option. Two independent iterations of two randomly selected trees were run until tree topologies converged. For iterations, average standard deviation of the split frequencies between the two trees was set to 0.005. Log-likelihood scores were plotted against generation time to determine when the Markov chains became stationary, with a "burn-in" value of 1000 selected for discarding generations. Trees resulting from the two iterations had identical tree topologies and posterior probabilities and were thus combined using the “sumt”

command to produce a single consensus tree, as recommended by Huelsenbeck and Ronquist (2001) and Ronquist and Huelsenbeck (2003).

Maximum likelihood (ML, Felsenstein 1981) phylogenetic analysis was conducted in PAUP* v4.0 beta 10 (Swofford, 2002), using the GTR+I+Γ model for nucleotide substitution. The GTR+I+Γ model was chosen because both the Akaike Inference Criterion (AIC, Akaike, 1974) and the Baysian Inference Criterion (BIC, Schwarz, 1978) provided in Modeltest 3.7 (Posada and Crandall, 1998) indicated it to best fit the data. The optimal ML tree was determined using a heuristic search with 100 random sequence additions and tree bisection reconnection (TBR). Bootstrap resampling incorporated a heuristic search of 1000 pseudoreplicates and near-neighbor interchange (NNI).

Genetic Algorithm for Rapid Likelihood Inference was run with GARLI v0.95 (Zwickli, 2006), using the GTR+I+Γ model for nucleotide substitution as recommended by Modeltest 3.7 (Posada and Crandall, 1998). Three independent tree constructions were conducted with random starting topologies. Bootstrap re-sampling included 100 pseudoreplicates with NNI branch swapping. Results were exported from GARLI to PAUP* v4.0 beta 10 for visualization of trees.

Maximum parsimony (MP) analysis was executed using PAUP* v4.0 beta 10 options for heuristic searching, TBR, and 1000 replicates. Bootstrap resampling was performed using 1000 pseudoreplicates and 10 random addition TBR.

Minimum evolution—maximum likelihood analysis (ME-ML) with GTR+I+Γ settings was performed in PAUP* v4.0 beta 10. The search was run using the heuristic setting with TBR swapping and 1000 replicates. Bootstrap resampling was as above for maximum parsimony analysis.

Lastly, a trace of the ciliate polymorphic character tree was accomplished using MacClade v4.05 (Maddison, D. and Maddison, W., 1989). Each taxon was coded as either zero (= non-polymorphic) or one (= polymorphic) before tracing the character on the maximum parsimony tree obtained above.

Results

Phylogenetic Analysis

SSU rRNA gene sequences for 64 species of ciliates (Table 2-1) were used in five separate phylogenetic analyses (GARLI Inference [GI], Baysian Inference [BI], maximum likelihood [ML], minimal evolution [ME], and maximum parsimony [MP]) to establish the placement of the subclass Scuticociliatia within the phylum Ciliophora and to assess relationships among polymorphic species of the Oligohymenophorea. Six of the sequences used in the analyses represent polymorphic Oligohymenophorea for which data were previously unavailable, while eight were original sequences for non-polymorphic scuticociliates. Data for the remaining 49 species were selected from GenBank/NCBI to ensure complete coverage of polymorphic Oligohymenophorea (2 additional species) and to include all available data for the subclasses Scuticociliatia (22 additional non-polymorphic species) and Astomatia (1 species). For the three remaining oligohymenophorean subclasses (Peritrichia, Peniculia, and Hymenostomatia), sequences of 7-10 species were chosen from Genbank to provide full representation of genera for which data were available. All analyses were conducted using the outgroup *Loxodes striatus* to root the trees.

Sequence lengths and guanine/cytosine (GC) percentages for sequences from all 64 species of ciliates used in the analyses are provided in Table 2-1. The final

length of the aligned nuclear SSU rRNA sequences was 1762 base pairs. The data set used for these analyses excluded hypervariable regions (total of 42 base pairs in length) that could not be aligned. Trees generated by the five phylogenetic analyses were of identical topology, but bootstrap values differed markedly at some nodes (Figure 2-1 and 2.2). The branch length for the GI tree was –ln=19264.18712. Tree scores for the ME and MP trees were 1.91061 and 4,185 steps, respectively.

All five analyses confirmed monophyly of both the Peritrichia (GI=100, ML=100, BI=1.0, ME=100, and MP=100) and the Hymenostomatia (GI=99, ML=98, BI=0.93, ME=99, and MP=58). Additionally, the Peritrichia and Hymenostomatia were consistently placed as sister subclasses with strong bootstrap support (GI=100, ML=100, BI=1.0, ME=100, and MP=100). Monophyly of the subclasses Scutiociliatia and Peniculia, as well as their placement within the Oligohymenophorea, were not well resolved, due largely to the placement of three taxa, the apostome *Anoplophrya marylandensis*, the scuticociliate *Dexitrichides pangi*, and the peniculine *Urocentrum turbo*. *Urocentrum turbo* and *Dexitrichides pangi* branched as sister taxa (GI=50, ML=52, BI=0.48, ME=41, and MP <50) intermediate to clades containing the other scuticociliates and other peniculines, respectively. *Urocentrum turbo* and *Dexitrichides pangi* were also separated from the larger scuticociliate cluster by the apostome *Anoplophrya marylandensis*.

Bootstrap support from the five analyses (GI=79, ML=59, BI=0.78, ME=99, and MP=93) supported the placement of all three polymorphic scuticociliates (*Miamiensis avidus* Strain MA/2, *Glauconema bermudiense*, and *Potomacus pottsi*) within the Parauronematidae. Also included within the Parauronematidae were four monomorphic taxa, *Mesanophrys carcini*, *Anophryoides haemophila*, *Miamiensis avidus* Strain MA, and *Philasterides dicentrarchi*.

The group formed by *M. avidus* Strain MA/2 and *A. haemophila* was sister to a cluster that includes two monomorphic scuticociliates (*Philasterides. dicentrarchi* and *M. avidus* Strain MA) and the polymorphic species *G. bermudiense* (GI= 68, ML=100, BI=1.0, ME=72, and MP=73). The *P. dicentrarchi*, *M. avidus* Strain MA, and *G. bermudiense* cluster were sister to the *Miamiensis avidus* Strain MA/2 and *Anophryoides haemophila*, which branched as polymorphic and monomorphic sister taxa (GI= 64, ML=76, BI=1.0, ME=92, and MP=65). The polymorphic ciliate *Potomacus pottsi* was inferred as the sister taxon to the larger clade containing *M. avidus* Strain MA/2, *A. haemophila*, *P. dicentrarchi*, *M. avidus* Strain MA, and *G. bermudiense* (GI=87, ML=86, BI=1.0, ME=77, and MP=67). Lastly, the placement of *Mesanophrys carcini* was unfixed and external to the other six parauronematid species (GI=55, ML=52, BI<50, ME<50, and MP<50).

Five polymorphic ciliates were placed in the subclass Hymenostomatia (Oligohymenophorea). Three of these species, *Tetrahymena vorax*, *Tetrahymena*

paravorax, and *Tetrahymena patula*, grouped into the family Tetrahymenidae, but did not form a monophyletic group. *Tetrahymena patula* and *Tetrahymena paravorax* grouped as sister species (GI=65, ML=64, BI=0.94, ME=83, and MP=56) in a clade containing *Tetrahymena australis*. *Tetrahymena vorax*, however, was placed in a separate clade containing the two monomorphic ciliates, *Tetrahymena canadensis* and *Tetrahymena farleyi* (GI=99, ML=98, BI=0.93, ME=99, and MP=58).

The two other polymorphic hymenostomes, *Ichthyophthirius multifiliis* and *Ophryoglena catenula*, were placed as sister taxa to each other (GI=65, ML=86, BI=0.97, ME=100, and MP=100) in the suborder Ichthyophthiridae and Ophryoglenidae. Separation of the polymorphic ophryoglenines from the polymorphic tetrahymeninines was supported by high bootstrap values (GI=99, ML=98, BI=0.93, ME=99, and MP=58).

A MacClade character trace using the maximum parsimony tree indicated that the polymorphic trait arose on at least four, and perhaps on as many as six, separate occasions within the oligohymenophorean ciliates (Figure 2-3). The number of origins in the Hymenostomatia was unambiguous and occurred on three separate occasions. Polymorphism arose, twice in the Tetrahymenidae, occurring within each of the two separate clades of polymorphic *Tetrahymena ssp*., (i.e., once in the *Tetrahymena patula*, *Tetrahymena paravorax* and *Tetrahymena australis* clade and once in the *Tetrahymena vorax*, *Tetrahymena canadensis* and *Tetrahymena farleyi*

clade). By contrast, polymorphism arose only once the Ophryoglenidae as the common ancestral trait in both *Ichthyophthirius multifiliis* and *Ophryoglena catenula*.

The number of origins of polymorphism in the Scuticociliatia, however, was ambiguous. The scuticociliates *Miamiensis avidus* Strain MA/2, *Glauconema bermudiense*, and *Potomacus pottsi* may have gained the polymorphic character on three separate occasions, with potentially one reversal in the Parauronematid *Anophryiodes haemophila*. Alternatively, the non-polymorphic scuticociliates *Miamiensis avidus* Strain MA, *A. haemophila* and *Philasterides dicentrarchi* may have obtained and secondarily lost the trait, because the number of evolutionary steps required for either loss or gain of polymorphism was the same (i.e., 3 in either case). Thus, the trait arose on at least one occasion and possibly as many as three separate occasions within the subclass Scuticociliatia. For the Oligohymenophorea as a whole, the character trace indicated that morphological polymorphism was acquired on at least four occasions and possibly on as many as six separate instances.

Table 2-1. American Type Culture Collection (ATCC) accession numbers, GC content, and SSU rRNA sequence length for ciliate taxa used in phylogenetic analyses.

Table 2-1. American Type Culture Collection (ATCC) accession numbers, GC content, and SSU rRNA sequence length for ciliate taxa used in phylogenetic analyses.

Taxon Name		GC Content	Sequence Length	ATCC Number
Hymenostomatia				
Hymenostomatida				
Tetrahymenidae				
	Tetrahymena paravorax	43%	1747	205177
	Tetrahymena patula	43.5%	1751	30769
	Tetrahymena vorax	43%	1748	304201
Scuticociliatia				
Philasterida				
Parauronematidae				
	Glauconema bermudiense	44%	1755bp	50160
	Potomacus pottsi	43.7%	1763bp	50190
	Parauronema acutum	44%	1756bp	50189
	Miamiensis avidus Strain Ma	43.7%	1763bp	50179
	Miamiensis avidus Strain Ma/2	44%	1761bp	50180
Philasteridae				
	Philasterides dicentrarchi	44%	1758bp	n/a
Pseudocohnilembidae				
	Pseudocohnilembus marinus	44%	1754bp	50208
Orchitophryidae				
	Anophryoides solidoi	43.6%	1748bp	50204
	Metanophrys diminuta Strain 34-1	44%	1754bp	50207
	Metanophrys diminuta Strain 1-1	44%	1753bp	50188
	Metanophrys diminuta Strain 19-3	43.6%	1749bp	50257
Uronematidae				
	Uronema falcificum	43.5%	1748bp	n/a

Table 2-2. Accession Numbers for Ciliate SSU rRNA Sequences Obtained from Genbank.

Table 2-2. Accession Numbers for Ciliate SSU rRNA Sequences Obtained from Genbank.

Taxon Name		Accession Number
Astomatia		
Astomatida		
Anoplophryidae		
	Anoplophrya marylandensis	AY547546
Peniculia		
Peniculida		
Frontoniidae		
	Apofrontonia dohrni	AM072621
	Frontonia lynii	DQ190463
	Frontonia tchibisovae	DQ885987
	Frontonia vernalis	U97110
Lembadionidae		
	Lembadion bullinum	AF255358
Parameciidae		
	Paramecium bursaria	AB219526
	Paramecium woodruffi	AF255362
Urocentridae		
	Urocentrum turbo	EF114300
Peritrichia		
Sessilida		
Epistylididae		
	Epistylis chrysemydis	AF335514
Lagenophryidae		
	Opercularia microdiscum	AF401525
Vaginicolidae		
	Vaginicola crystallina	AF401521
Vorticellidae		
	Carchesium polypinum	AB074079
	Vorticella campanula	DQ662849
Zoothamniidae		
	Zoothamnium crystallina	DQ868353
	Zoothamnium pelagicum	DQ868351
Hymenostomatia		
Hymenostomatida		
Glaucomidae		
	Glaucoma chattoni	AJ810075
	Bromeliophrya basiliensis	AJ810075
Ichthyophthiriidae		
	Ichthyophthirius multifiliis	U17354
Ophryoglenidae		
	Ophryoglena catenula	U17355
Tetrahymenidae		
	Tetrahymena australis	X56167
	Tetrahymena bergeri	AF364039
	Tetrahymena canadensis	X56170
	Tetrahymena epidokyrea	U36222
	Tetrahymena farleyi	AF184665

Turaniellidae		
	Colpidium campylum	X56532
Scuticociliatia		
Philasterida		
Cohnilembidae		
	Cohnilembus verminus	Z22872
Entodiscidae		
	Entodiscus borealis	AY541687
Entorhipidiidae		
	Entorhipidium tenue	AY541688
	Entorhipidium triangularis	AY541690
Parauronematidae		
	Parauronema longum	AY212807
Pseudocohnilembidae		
	Pseudocohnilembus hargisi	AY833087
	Pseudocohnilembus persalinus	AY835669
Loxocephalidae		
	Cardiostomatella veriforme	AY881632
	Dexitrichides pangi	AY212805
Orchitophryidae		
	Anophryoides haemophila	AHU51554
	Mesanophrys carcini	AY103189
	Metanophrys similis	AY314803
	Paranophrys magna	AY103191
Schizocarydae		
	Schizocaryum dogieli	AF527756
Thyrophyclacidae		
	Plagiopyliella pacifica	AY541685
	Thyrophylax vorax	AY541686
Uronematidae		
	Uronema elegans	AY103190
	Uronema marinum	AY551905
Pleuronematida		
Cyclidiidae		
	Cyclidium glaucoma	Z22879
	Cyclidium plouneouri	U27816
Pleuronematidae		
	Pleuronema coronatum	AY103188
	Schizocalyptra aeschtae	DQ777744

Figure 2-1. Phylogenetic relationships for the Oligohymenophorea determined by GARLI likelihood inference, Bayesian inference, and maximum likelihood analysis of nuclear small subunit rRNA sequences. A relative phylogram for GARLI likelihood inference tree (GI -ln=19264.18712), Baysian inference, and maximum likelihood analyses of 63 Oligohymenophorean species, with the karyorelictean *Loxodes striatus* as the outgroup, is presented on the left. Values listed at nodes are GARLI bootstrap values/maximum likelihood bootstrap values/Bayesian posterior probabilities. An asterisk '*' denotes bootstrap values below 50%. A phylogram with true branch lengths is presented on the right. Branch lengths are mean values and are proportional to the number of substitutions per site. (scale bar = 0.05 substitutions/site). Red text indicates polymorphic organisms. Blue text indicates either endo- or ectoparasites. Green text indicates sessile filter feeding bacteriovores. Black text indicates free-living bacteriovores. Subclass = s.c.; order = o.; family = f. Ordinal separations also indicated by horizontal while lines.

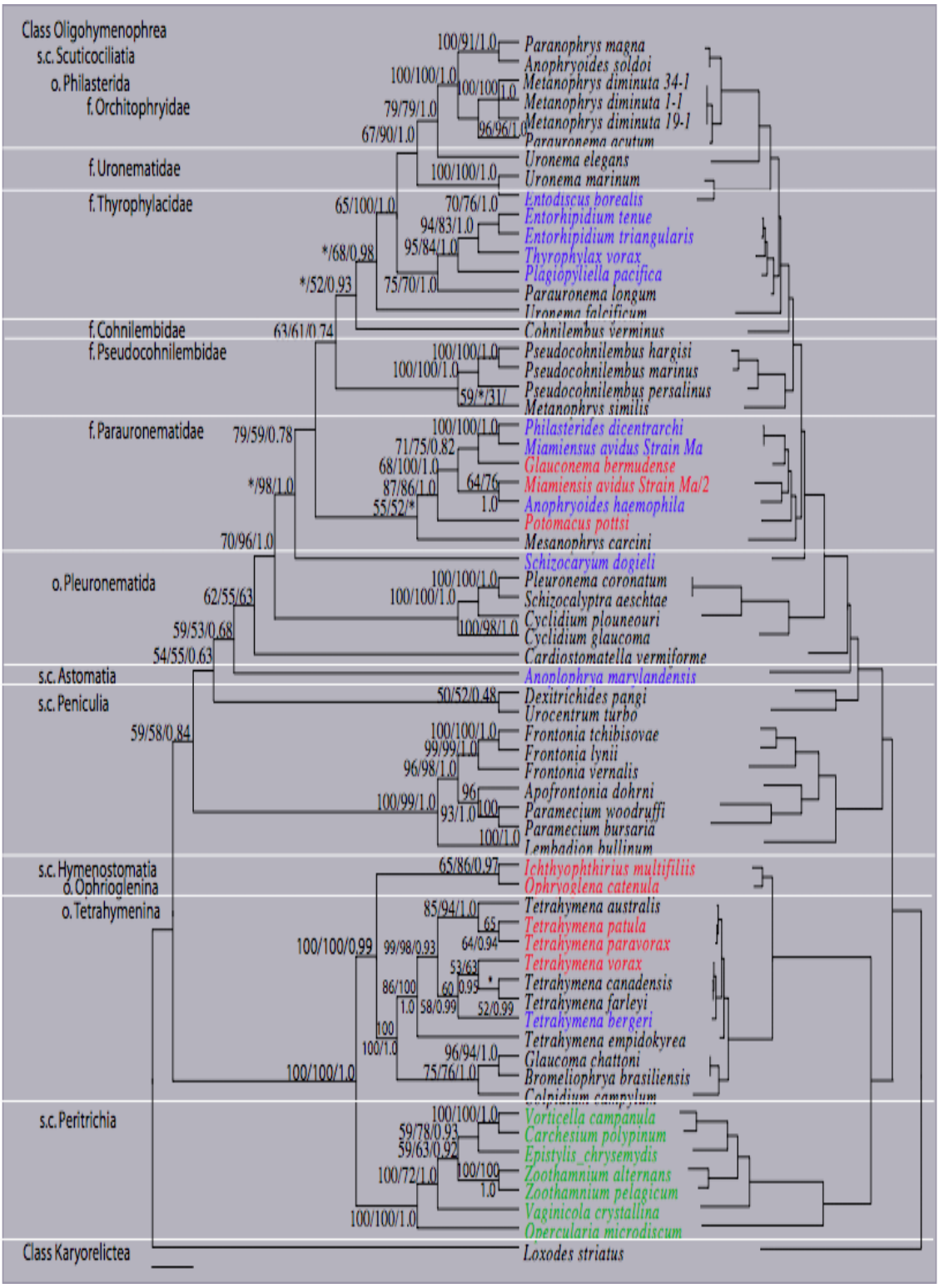
Class Oligohymenophrea
s.c. Scuticociliatia
o. Philasterida
f. Orchitophryidae
f. Uronematidae
f. Thyrophylacidae
f. Cohnilembidae
f. Pseudocohnilembidae
f. Parauronematidae
o. Pleuronematida
s.c. Astomatia
s.c. Peniculia
s.c. Hymenostomatia
o. Ophrioglenina
o. Tetrahymenina
s.c. Peritrichia
Class Karyorelictea
Paranophrys magna
Anophryoides soldoi
Metanophrys diminuta 34-1
Metanophrys diminuta 1-1
Metanophrys diminuta 19-1
Parauronema acutum
Uronema elegans
Uronema marinum
Entodiscus borealis
Entorhipidium tenue
Entorhipidium triangularis
Thyrophylax vorax
Plagiopyliella pacifica
Parauronema longum
Uronema falcificum
Cohnilembus verminus
Pseudocohnilembus hargisi
Pseudocohnilembus marinus
Pseudocohnilembus persalinus
Metanophrys similis
Philasterides dicentrarchi
Miamiensus avidus Strain Ma
Glauconema bermudense
Miamiensis avidus Strain Ma/2
Anophryoides haemophila
Potomacus pottsi
Mesanophrys carcini
Schizocaryum dogieli
Pleuronema coronatum
Schizocalyptra aeschtae
Cyclidium plouneouri
Cyclidium glaucoma
Cardiostomatella vermiforme
Anoplophrya marylandensis
Dexitrichides pangi
Urocentrum turbo
Frontonia tchibisovae
Frontonia lynii
Frontonia vernalis
Apofrontonia dohrni
Paramecium woodruffi
Paramecium bursaria
Lembadion bullinum
Ichthyophthirius multifiliis
Ophryoglena catenula
Tetrahymena australis
Tetrahymena patula
Tetrahymena paravorax
Tetrahymena vorax
Tetrahymena canadensis
Tetrahymena farleyi
Tetrahymena bergeri
Tetrahymena empidokyrea
Glaucoma chattoni
Bromeliophrya brasiliensis
Colpidium campylum
Vorticella campanula
Carchesium polypinum
Epistylis_chrysemydis
Zoothamnium alternans
Zoothamnium pelagicum
Vaginicola crystallina
Opercularia microdiscum
Loxodes striatus

Figure 2-2. Phylogenetic relationships for the Oligohymenophorea determined by maximum parsimony and minimum evolution (GTR+I+Γ) analysis of nuclear small subunit rRNA sequences. A relative phylogram for maximum parsimony (tree score = 1.91061) and minimum evolution (tree score = 4,185 steps) analyses of 63 Oligohymenophorean species, with the karyorelictean *Loxodes striatus* as the outgroup, is presented on the left. Bootstrap values are listed at nodes for maximum parsimony/minimum evolution. A phylogram with true branch lengths is presented on the right. Branch lengths are mean values and are proportional to the number of substitutions per site (scale bar = 0.05 substitutions/site). Red text indicates polymorphic organisms. Blue text indicates either endo- or ectoparasites. Green text indicates sessile filter feeding bacteriovores. Black text indicates free-living bacteriovores. Subclass = s.c.; order = o.; family = f. Ordinal separations also indicated by horizontal while lines.

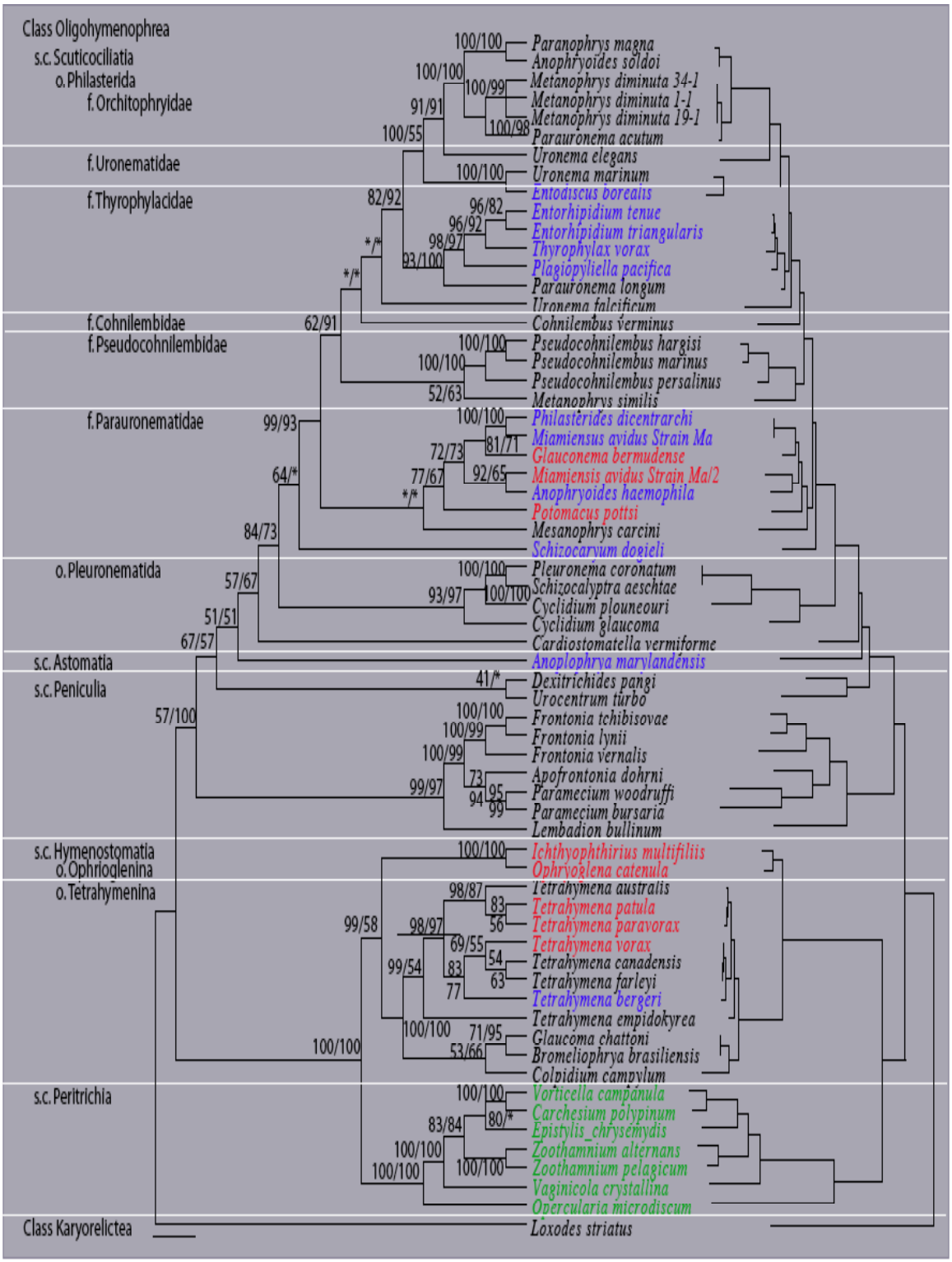
Class Oligohymenophrea
s.c. Scuticociliatia
o. Philasterida
f. Orchitophryidae
f. Uronematidae
f. Thyrophylacidae
f. Cohnilembidae
f. Pseudocohnilembidae
f. Parauronematidae
o. Pleuronematida
s.c. Astomatia
s.c. Peniculia
s.c. Hymenostomatia
o. Ophrioglenina
o. Tetrahymenina
s.c. Peritrichia
Class Karyorelictea
Paranophrys magna
Anophryoides soldoi
Metanophrys diminuta 34-1
Metanophrys diminuta 1-1
Metanophrys diminuta 19-1
Parauronema acutum
Uronema elegans
Uronema marinum
Entodiscus borealis
Entorhipidium tenue
Entorhipidium triangularis
Thyrophylax vorax
Plagiopyliella pacifica
Parauronema longum
Uronema falcificum
Cohnilembus verminus
Pseudocohnilembus hargisi
Pseudocohnilembus marinus
Pseudocohnilembus persalinus
Metanophrys similis
Philasterides dicentrarchi
Miamiensus avidus Strain Ma
Glauconema bermudense
Miamiensis avidus Strain Ma/2
Anophryoides haemophila
Potomacus pottsi
Mesanophrys carcini
Schizocaryum dogieli
Pleuronema coronatum
Schizocalyptra aeschtae
Cyclidium plouneouri
Cyclidium glaucoma
Cardiostomatella vermiforme
Anoplophrya marylandensis
Dexitrichides pangi
Urocentrum turbo
Frontonia tchibisovae
Frontonia lynii
Frontonia vernalis
Apofrontonia dohrni
Paramecium woodruffi
Paramecium bursaria
Lembadion bullinum
Ichthyophthirius multifiliis
Ophryoglena catenula
Tetrahymena australis
Tetrahymena patula
Tetrahymena paravorax
Tetrahymena vorax
Tetrahymena canadensis
Tetrahymena farleyi
Tetrahymena bergeri
Tetrahymena empidokyrea
Glaucoma chattoni
Bromeliophrya brasiliensis
Colpidium campylum
Vorticella campanula
Carchesium polypinum
Epistylis_chrysemydis
Zoothamnium alternans
Zoothamnium pelagicum
Vaginicola crystallina
Opercularia microdiscum
Loxodes striatus

Figure 2-3. Character trace of morphological polymorphism within the Oligohymenophorea. The polymorphic trait was constructed with the maximum parsimony tree of Figure 2-2. Origins and deletions of the character are indicated by blue and red lines, respectively. (a) Origins and deletions within the Scuticociliatia. (b) Origins within the Hymenostomatia.

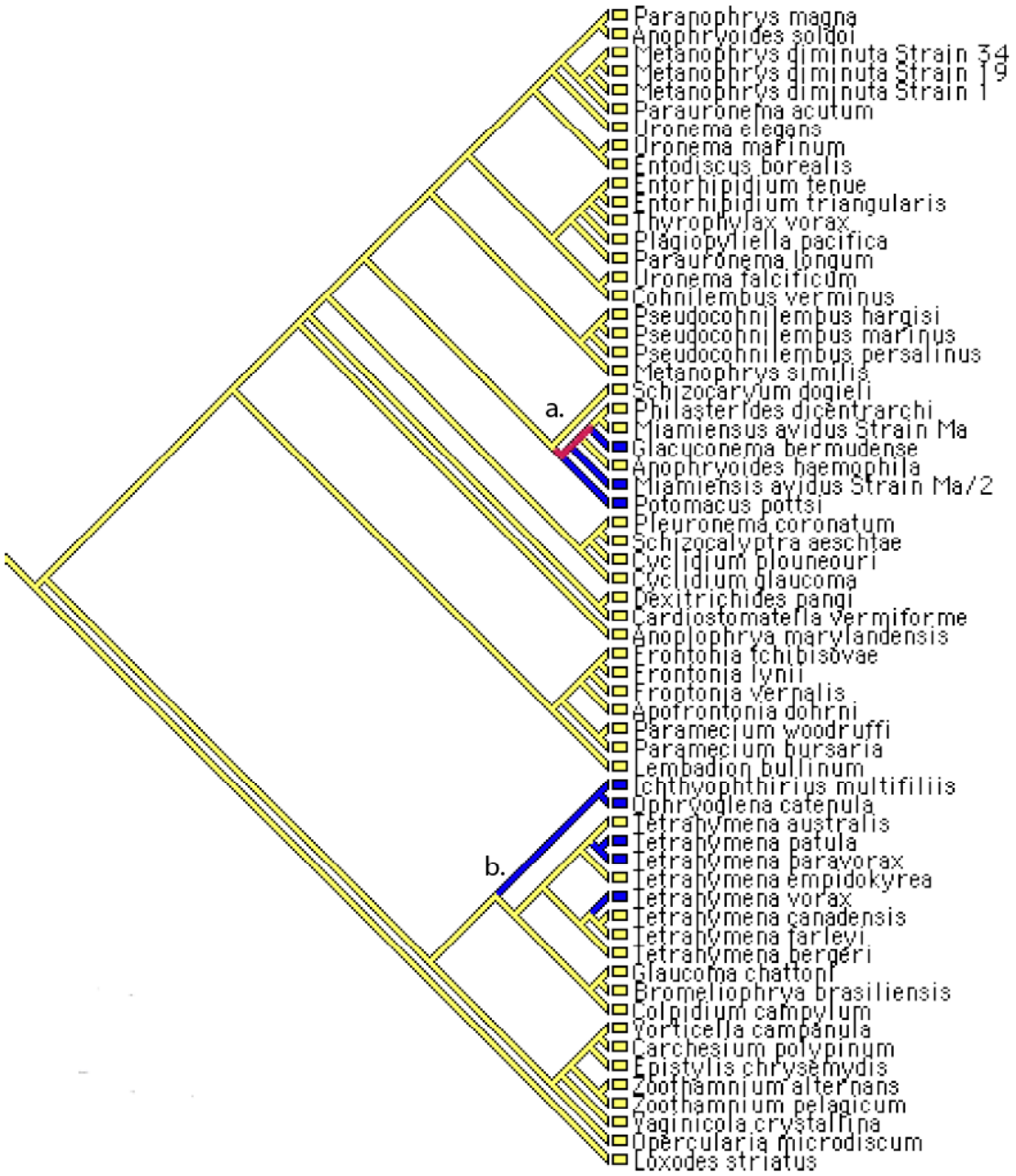
Paranophrys magna
Anophryoides soldoi
Metanophrys diminuta Strain 34
Metanophrys diminuta Strain 19
Metanophrys diminuta Strain 1
Parauronema acutum
Uronema elegans
Uronema marinum
Entodiscus borealis
Entorhipidium tenue
Entorhipidium triangularis
Thyrophylax vorax
Plagiopyliella pacifica
Parauronema longum
Uronema falcificum
Cohnilembus verminus
Pseudocohnilembus hargisi
Pseudocohnilembus marinus
Pseudocohnilembus persalinus
Metanophrys similis
Schizocaryum dogieli
Philasterides dicentrarchi
Miamiensus avidus Strain Ma
Glaucomena bermudense
Anophryoides haemophila
Miamiensis avidus Strain Ma/2
Potomacus pottsi
Pleuronema coronatum
Schizocalyptra aeschtae
Cyclidium plouneouri
Cyclidium glaucoma
Dexitrichides pangi
Cardiostomatella vermiforme
Anoplophrya marylandensis
Frontonia fchibisovae
Frontonia lynii
Frontonia vernalis
Apofrontonia dohrni
Paramecium woodruffi
Paramecium bursaria
Lembadion bullinum
Ichthyophthirius multifiliis
Ophryoglena catenula
Tetrahymena australis
Tetrahymena patula
Tetrahymena paravorax
Tetrahymena empidokyrea
Tetrahymena vorax
Tetrahymena canadensis
Tetrahymena farlevi
Tetrahymena bergeri
Glaucoma chattoni
Bromeliophrya brasiliensis
Colpidium campylum
Vorticella campanula
Carchesium polypinum
Epistylis chrysemydis
Zoothamnium alternans
Zoothamnium pelagicum
Vaginicola crystallina
Opercularia microdiscum
Loxodes striatus
a.
b.

Discussion

Phylogenetic Relationships within the Class Oligohymenophorea

Statistical testing of tree topologies failed to support monophyly all subclasses (the Hymenostomatia, Peritrichia, Peniculia, Apostomatia, Astomatia, and Scuticociliatia) within the Class Oligohymenophorea. At present, too few sequences are available to test monophyly of the astomes, and no sequences are available for apostomes. The analyses presented here generally confirmed the monophyletic relationships for the Hymenostomatia and Peritrichia, as reported elsewhere (Sogin, 1986; Struder-Kypke, 2000; Struder-Kypke 2001; Utz and Eizirik, 2007; and Wei Miao 2004). However, the monophyletic Peniculia and Scuticociliatia included most, but not all, taxa for which SSU gene sequences were examined.

The placement of *Urocentrum turbo* within the Peniculia was problematic for this study and others (Struder-Kypke et al., 2000). The maximum likelihood analysis of Struder -Kypke et al., (2000) placed *U. turbo* within an unresolved clade that included six scuticociliate taxa. In my analyses, *U. turbo* clustered basal to the scuticociliatia with improved resolution. The improved resolution between *U. turbo* and the Scuticiociliate clade was most likely due to refinement of the sequence evolution model used in my maximum likelihood and Bayesian analyses. Struder-Kypke et al. (2000) used differences in the secondary structure of the SSU rRNA

molecule and morphological characters (the method of stomatogenesis and the peniculine spindle toxocysts) to divide the Subclass Peniculia into two orders, the Urocentrida and the Peniculida. My analyses did not support this relationship, but instead placed the Urocentridae outside of the monophyletic Peniculia. Additional *U. turbo* SSU rRNA sequences are required to resolve the placement of this enigmatic genus.

Phylogenetic Relationship of the Subclass Scuticociliatia

Another aim of this study was to test the monophyly of the subclass Scuticociliatia. Statistical testing of tree topologies supported the general phylogenetic scheme of Lynn and Small (2000) and Small (1967), which elevated the Scuticociliatia to the subclass level and established the orders Philasterida and the Pleuronematida, and Thigmotrichida. The ambiguous placement of several taxa within the Scuticociliatia reduced the likelihood that the subclass formed a monophyletic group. For example, the astome *Anoplophrya marylandensis* consistently clustered with the pleuronematine scuticociliates, separating the scuticociliate *Dexitrichides pangi* from the larger scuticociliate clade. Support for placement of *Anoplophrya marylandensis* at the base of the Scuticociliate clade was ambiguous. However, others have proposed hypotheses placing the astomes ancestral to the thigmotrich scuticociliates. This hypothesis is based on morphological similarity between the mouthless astomes and thigmotrichs that undergo dramatic oral

reduction at times during their life-history (Affa'a et al., 2004; Corliss, 1979, du Puytorac, 1974; Grain and Groliere, 1979). Future studies using thigmotrich and additional astome SSU gene sequences should be used to test hypotheses concerning the phylogenetic relationship between these two elusive groups of taxa.

Additionally, there were several problematic taxa where placement in scuticociliate families contradicted accepted phylogenies based on morphological characters (Lynn and Small, 2000; Small and Lynn, 1985; Small 1967). For example, three species of *Metanophrys* clustered within the family Orchitophryidae, in keeping with the phylogenetic scheme of Lynn and Small 2000, while *Metanophrys similis,* clustered within a different family, the Pseudocohnilembidae. The placement of *Uronema falcificum* in the Thyrophylacidae rather than in the Uronematidae and inclusion of *Mesanophrys carcini* within the Parauronematidae instead of the Orchitophryidae also contradicted accepted morphological schemes for the Scuticociliatia (Lynn and Small, 2000; Small and Lynn, 1985; Small 1967).

Phylogenetic Relationship of Polymorphic and Non-Polymorphic Taxa within the Oligohymenophorea

Recent morphological schemes place polymorphic taxa (e.g. oral replacement) in two distinct subclasses of Oligohymenophorea, which also included non-polymorphic taxa (Corliss, 1974; Lynn and Small, 2000; Small and Lynn, 1985; Small 1967). Molecular data provided here support placement of the polymorphic scuticociliates

within the Parauronematidae and hymenostomes in the Tetrahymenida, Ichthyophthiridae, and Ophryoglenidae, supporting the phylogenetic scheme of Lynn and Small (2000). SSU rRNA gene sequences for polymorphic taxa were used to evaluate hypotheses concerning the monophyly of the polymorphic Scucticociliatia and Hymenostomatia. A character map was traced onto the maximum parsimony tree using polymorphic versus non-polymorphic character states to test broader hypotheses concerning the number of polymorphic losses or gains. Combined phylogenetic analyses and the character map suggest a trend towards loss of the polymorphic trait within the Scuticociliatia and gain in the Oligohymenophorea.

Analysis of the SSU rRNA sequences placed the polymorphic scuticociliate, *Potomacus pottsi,* at the base of the Parauronematidae. This basal placement of *P. pottsi* is enigmatic considering that it has the most complex scuticociliate life history stages, including one tomite and two distinct microstome and macrostome stages (five total stages) within its respective life history (Ramsey 1981, Ramsey et al. 1980; Thompson 1966). If *P. pottsi* is the closest common ancestor to the remaining Parauronematidae then all derived taxa should share the polymorphic trait (assuming it has not been lost yet). However, *P. pottsi* is basal to the cluster that includes the polymorphic *M. avidus* Strain Ma/2 and the non-polymorphic *Anophryoides haemophila. M. avidus* Strain Ma/2 has a tomite, and single microstome and macrostome morphologies (three total stages) and may have independently gained polymorphic stages, while *A. haemophila* may have recently lost the trait. Neither

analysis resolved this particular ambiguity because the likelihood or number of steps for loss or gain was the same for both outcomes. If *M. avidus* Strain Ma/2 gained the trait it would represent the second polyphyletic gain. Accordingly, *A. haemophila* may be the first taxa to loose the polymorphic character.

Additionally, *Miamiensis avidus* Strain Ma/2 and *Anophryoides haemophila* were a sister group to the cluster containing *Philasterides dicentrarchi, Miamiensis avidus* Strain Ma and *Glauconema bermudiense* (Gomez-Saladin and Small, 1993a-c; Moewus, 1962; Ragan et al., 1996; Thompson and Moewus, 1964). *G. bermudiense,* a species that has microstomes and tomites, but not macrostomes (two total stages), was basal to the most recently derived non-polymorphic *P. dicentrarchi* and *M. avidus Strain* Ma cluster (Small et al., 1986).

Thus, the extant Parauronematidae may have evolved from a common ancestor that originated in a marine environment, had five life-history stages, and more recently lost three life-history stages. Alternatively, the three polymorphic scuticociliates may represent taxa that independently gained the polymorphic character. The phylogenetic analyses and the character trace supported the former interpretation, while only the character trace provides evidence for the latter.

The polymorphic hymenostomes *Tetrahymena vorax, Tetrahymena paravorax,* and *Tetrahymena patula* clustered on two separate branches within the monphyletic

Tetrahymenidae, confirming the relationships among tetrahymenines as provided in earlier works (Struder-Kypke 2000). *Tetrahymena vorax* and *Tetrahymena paravorax* have microstomes and macrostomes, while *Tetrahymena patula* has a tomite (derived from a division cyst) in addition to microstome and macrostome stages (Corliss, 1972; Williams, 1961; Williams et al. 1992). One group of tetrahymenines included *Tetrahymena paravorax* and *Tetrahymena patula* and was inferred as the sister taxon to a second group of tetrahymenines containing *Tetrahymena vorax.* Both tetrahymenine clusters were more recently derived than the basal non-polymorphic *T. empidokrea* (based on tree branch length). The hypothesis that the common ancestor to the tetrahymenines was a polymorphic taxon and that this trait was lost in the larger tetrahymenine cluster was rejected. For the most common ancestor to have been polymorphic would require loss of the trait in *T. empidokrea* and others, reacquisition in *T. vorax, T. paravorax,* and *T. patula,* and then subsequent loss in two separate branches that include both polymorphic and non-polymorphic taxa (the *T. australis, T. patula,* and *T. paravorax* clade and the *T. vorax, T. canadensis, T. farleyi,* and *T. bergeri* clade). Thus, the hypothesis that polymorphic trait most likely evolved on two separate occasions within the Tetrahymenidae was accepted.

Lastly, the *Ichthyophthirius multifiliis* and *Ophryoglena catenula* were placed within the sister families Ichthyophthiridae and Ophryoglenidae, respectively. The phylogenetic analyses and the character trace suggest that the Ichthyophthiridae and Ophryoglenidae cluster basal to and evolved independently from the polymorphic

Tetrahymenidae. The statistical support for tree topologies and the character trace supports the hypothesis that the polymorphic trait was gained once within Ichthyophthiridae and Ophryoglenidae clade. The polymorphic trait was gained on three separate occasions within the monophyletic Hymenostomatia. Thus, the polymorphic trait was gained on at least four, and perhaps on as many as six times, or may have been lost on two separate occasions within the oligohymenophorean ciliates.

Summary

Previous phylogenetic reconstruction of the Oligohymenophorea relied exclusively on morphological characters that include ciliary fibers and microtubule structures and methods of divisional stomatogenesis (Corliss, 1979; Lynn and Small, 2000; Small and Lynn, 1985). This study used known scuticociliate SSU rRNA genes sequences coupled with other sequences to conduct a robust phylogenetic analysis of the class Oligohymenophorea. The Hymenostomatia, Peritrichia, Scuticociliatia and the Peniculia represent monophyletic subclasses, some of which included most but not all taxa. At present, there is a paucity of sequences available to test monophyly of the astomes, and virtually no sequences for apostomes. Obtaining gene sequences from these three groups presents a challenge concerning species identification and DNA isolation from metazoan host tissues. This is extremely difficult given that some apostomes have not been isolated since the designation of their species provided in their original description.

Many Scuticociliate taxa have been analyzed and confirm the general phylogenetic scheme of Lynn and Small (2002), such as the Scuticociliatia and the orders Philasterida and the Pleuronematida. Several scuticociliate taxa contradict generally accepted phylogenetic schemes based on morphology and as such should be re-isolated, reanalyzed, and spurious relationships ultimately resolved. Molecular data

provided in this study supports placement of polymorphic scuticociliates within the family Parauronematidae and the placement of hymenostomes in the families Tetrahymenida, Ichthyophthiridae, and Ophryoglenidae, supporting the phylogenetic scheme of Lynn and Small (2002).

Although the exact number of gains or losses of polymorphism is unclear, monophyly of the scuticociliate family, the Parauronematidae including polymorphic and non-polymorphic taxa (excluding *Mesanophrys carcini*), should be accepted. The phylogenetic analyses and character trace suggest a trend towards loss of the polymorphic trait within the Scuticociliatia and gain in the Oligohymenophorea. The character map failed to support hypotheses of multiple origins within Scuticociliatia due to the three parsimonious steps that remained constant regardless of character loss or gain. However, the phylogenetic analysis and character map support broad hypotheses of polymorphic losses within the Scucitcociliatia. These results also confirm multiple polymorphic gains within Hymenosotmatia. Thus, the polymorphic trait originated at least four, and perhaps as many as six, separate occasions with respective losses and gains of the polymorphic character within the oligohymenophorean ciliates.

Chapter 3: Differential Expression of Genes During Morphological Transformation of the Parasitic Ciliate Miamiensis avidus Strain Ma/2

Abstract

Several free-living species of oligohymenophorean ciliates, including *Miamiensis avidus*, exhibit polymorphic life-cycles in which the transition from one life-history stage to another is cued by the quantity and quality of food. Three distinct life-history stages are recognized for *M. avidus*: a bacteriovorous microstome, a predatory macrostome, and a non-feeding tomite. While cellular signaling and signal interpretation has been addressed in *M. avidus* and other polymorphic Oligohymenophorea, little attention has been given to gene expression during transformation. Here I tested the hypothesis that genes are differentially expressed during microstome-to-macrostome and tomite-to-microstome transformation. Poly (A) mRNA was extracted from transforming populations was used to create two suppression subtraction hybridization libraries. After differential screening and sequence analysis, seven genes previously implicated in cell-cycle control and morphogenetic processes in eukaryotes were identified from *M. avidus* undergoing microstome-to-macrostome transformation. Those genes were, elongation factor-1 alpha (*Ef-1*α), a disulfide isomerase, heat shock protein 70, step II splicing factor (*Slu7*), U1 zinc finger, WD40-16 repeat, and encoding a Constans, Constans-like &

TOC1 (CCT) transcription factor. A similar analysis for *M. avidus* undergoing tomite-to-microstome transformation identified five genes previously linked to transformation processes in other protists: two cysteine protease genes lacking formal description (papain-family cysteine protease and *XCP1* cysteine protease), two described cysteine protease genes, cathepsin B and cathepsin L, and one cysteine protease inhibitor (cystatin-1) gene. The roles of three candidate genes for regulation of *M. avidus* life-history stages (*Ef-1*α for microstome-to-macrostome transformation; cathepsin B and cathepsin L for tomite-to-microstome transformation) were examined using pharmacological inhibition experiments. Inhibition of *Ef-1*α using *Lactacystin* significantly reduced transformation of *M. avidus* microstomes into macrostomes within 6 h. Similarly, treatment with two cysteine protease inhibitors, *E64* and *Leupeptin,* for 2.5 h significantly blocked tomite-to-microstome transformation in *M. avidus*. Results indicated that genes specifically linked to oral transformation in *M. avidus* are differentially expressed during microstome-macrostome and tomite-microstome transformation.

Introduction

Ciliated protists have long been used as model systems for understanding cell structure and function (Corliss, 1979; Fauré-Fremiet, 1950; Lynn and Small, 2000; Small and Lynn, 1985; Small et al., 1986), as they exhibit a diverse array of morphogenetic process that can be experimentally regulated. Their complex morphologies and short generation times provide opportunities for exploring nuclear, somatic, and cortical events associated with cell division (Corliss, 1979; Hausmann, 1996; Hausmann, 2003; Lynn and Small 2000). In addition, many species have complex life-histories manifesting distinct morphologies that respond to environmental cues. The polymorphic character of those life histories has been used to explore questions related to cellular signaling (Buchmann et al., 1999; Buhse et al., 1967; Butzel et al., 1983; Gomez-Saladin and Small 1993a-c), signal interpretation, (Lennartz et al., 1980; Ryals et al., 1999), and expression of genes relative to alterations of morphology (Villalobo, 2003).

Polymorphic ciliates are genetically identical organisms that express alternative phenotypes as component steps during their life histories and/or in response to changing environmental conditions (Fenchel 1987). In some instances, alternative phenotypes are not clearly linked to environmental cues. For example, reproductive buds occur in the Suctoria and are an obligate part of the asexual cycle chonotrichs (Corliss 1956; Curry 1982; Fox et al., 1992; Moher et al., 1970). Buds produced by

those ciliates are not only the sole means of asexual reproduction, but also serve as dispersal stages capable of colonizing new substrate. Similarly, digestive and division cysts common in hymenostome ciliates (Gabe and De Bault, 1973; Tokuyasu and Sherbaum, 1965) are required steps in the life cycle that appear independent of the environment. Many of the other alternative phenotypes present in ciliates, however, are expressed in response to changing environmental conditions. For example, *Euplotes ssp*. form short-lived resting cysts when prey is depleted (Rawlinson, 1986), while *Colpoda ssp*. produce desiccation-resistant cysts to persist during dry seasons (Foissner, 1993). Changes in phenotype can also be triggered by the presence of predators, or by metabolic shifts in host organisms. For example, *Onchyodromus quadricornutus* and other spirotrich ciliates develop large cytostomes and long dorsolateral spines to avoid predation by ciliates (Wicklow 1988), while apostomes transition between motile feeding stages and encysted non-feeding stages depending on ecdysis of their crustacean hosts (Bradbury, 1966; Bradbury, 1989; Landers 2006). Lastly, unfavorable environmental conditions can trigger peritrichs to form asexual dispersal cells (i.e., telotrochs), or micro- and macro-conjugants as part of their asexual cycle (Viljoen and Van As 1987; Grell 1973; Clamp and Coats 2000; others).

Several free-living species of oligohymenophorean ciliates exhibit polymorphic life-cycles in which the transition from one life-history stage to another is cued by the quantity and quality of food. While subtle differences in life-cycle occur in a few species, most of these species have three morphologically distinct

swimming stages: a bacteriovorous microstome, a predatory macrostome, and a non-feeding tomite [e.g., the hymenostomes, *Tetrahymena patula*, *Ichthyophthirius multifiliis*, and *Ophryoglena catenula* (Corliss, 1972; Hoffman, 1975; Savoie 1962) and the scuticociliates *Potomacus pottsi* and *Miamiensis avidus* Strain Ma/2 (Gomez-Saladin 1993a-c; Moewus, 1962; Ramsey, 1980a-b; Thompson, 1966)]. Microstomes and macrostomes are also known for *Tetrahymena vorax* and *Tetrahymena paravorax*, but those species appear to lack tomites (Corliss, 1971; and William et al. 1992). By contrast, microstomes and tomites, but not macrostomes have been reported for *Glauconema bermudiense* (Small et al. 1986). Digestion/division cysts are formed by the macrostomes of some of the species (Stone et al., 1964).

Transformation between life-history stages has been extensively examined using cultures of *M. avidus* (Gomez-Saladin 1993a-c). In *M. avidus*, microstomes are the most prevalent morphotype during log-growth. These cells are medium in size, have a small oral region (~ 1/4 total cell length), and possess three polykineties and a dikinety for sweeping bacteria to the cytostome-cytopharynx. The cytoplasm of microstomes is typically filled with small food vacuoles. When grown in the presence of *Paranophrys sp.* or other ciliate prey, microstomes of *M. avidus* undergo oral replacement to produce macrostomes. During oral replacement, the parental microstome oral apparatus is completely dedifferentiated and a new macrostome oral apparatus is formed from kinetosomes of an oral anlage derived from parental structures. Macrostomes are large predatory cells having an oral region that extends

~2/3 total cell length. The oral polykineties are slightly larger than in microstomes, but the oral dikinety is ~ 10 time longer. Macrostomes also have a large preparatory vacuole at the base of the cytostome-cytopharynx, enabling rapid ingestion of prey. Microstome-to-macrostome transformation also occurs in *M. avidus* cultures (typically mid to late log-growth phase) when microstome densities become high. When ciliate prey are not abundant, macrostomes transform to microstomes by cell division involving replacement of macrostome feeding structures. When bacterial prey is depleted, microstomes of *M. avidus* transform into tomites via oral reduction. The process of oral reduction is not well characterized, but results in cells that lack oral membranelles (polykineties and dikineties), or lack discernable oral regions. Tomites are small, fast swimming cells believed to be dispersal stages in search of prey. When bacterial prey is encountered, tomites transform into microstomes by elaboration of new oral structures.

While the quality and quantity of prey are known to stimulate morphological transformation in *M. avidus* and other polymorphic Oligohymenophorea, little is known about the chemical nature of signals involved in the processes. That chemical signals can trigger transformation, however, seems clear, as transferring microstomes of *Miamiensis avidus* and *Tetrahymena vorax* to prey-conditioned media promotes oral replacement and macrostome formation (Buhse, 1967; Gomez-Saladin, 1993b). Further, Buhse (1967) purified a peptide, termed stomatin, which was shown to be the chemical responsible for microstome-to-macrostome in *Tetrahymena vorax* Strain

V_2S. No studies have examined gene expression during morphological transformation in oligohymenophorean ciliates. Thus far, gene expression during ciliate transformation has only been examined by (Villalobo, 2003) during his study of encystment in stichotrich ciliate *Sterkiella histriomuscorum*.

Here, gene expression was examined during transformation of *Miamiensis avidus* cultures during the microstome-to-macrostome and tomite-to-microstome. Using a suppression subtraction hybridization (SSH) procedure, a set of differentially expressed genes was identified for each transformation. The roles of three candidate genes, one for the microstome-to-macrostome transformation and two for the tomite-to-microstome, were examined using a set of pharmalogical inhibition experiments and shown to be linked to oral transformation in *M. avidus*.

Materials and Methods

Ciliate Cultures

The scuticociliates *Miamiensis avidus* Strain Ma/2 (ATTC 50180) and *Paranophrys sp.* Strain 1-1 (ATCC 50188), a prey ciliate that induces microstome-to-macrostome transformation in *Miamiensis avidus*, were obtained from the American Type Culture Collection (ATCC, Manassas, VA, USA). They were cultivated axenically in 200-ml volumes of MA1651 saline nutrient medium (ATCC, Manassas, VA, USA). All cultures were incubated at 25 °C in the dark and transferred to fresh medium at 2-week intervals. Cultures were propagated to multiple flasks as necessary for experiments. To assure that cultures remained axenic, an aliquot was removed weekly from each culture and plated on nutrient agar (Fisher Scientific, Pittsburgh, PA, USA #S71613). Agar plates were incubated at 37 °C to for two days to allow growth and detection of possible bacterial contaminants. Subcultures that showed bacterial contamination were discarded.

Microstome to Macrostome Transformation

Ten 200-ml stock cultures of *Paranophrys sp.* Strain 1-1 were maintained in log-growth until cell densities reached ~2.5 X 10^5 cells/ml. The *Paranophrys sp.* cells were aseptically separated from MA1651 growth medium by vacuum filtration using

1-liter, 0.22-μm Millipore filter unit (Millipore, Billerica, MA, USA #SCGV U11RE). The resulting 2 liters of filtrate (=prey-conditioned medium) contained the factors necessary for inducing microstome-to-macrostome transformation in *M. avidus* (Gomez-Saladin, 1993c; Buhse, 1967).

A 1-ml aliquot from each of 20 200-ml stock cultures of *M. avidus* microstomes (i.e., log-growth cells at ~ 2.5 X 10^5 cells/ml) was preserved with Bouin's fixative (Montagnes and Lynn 1993) for determination of cell densities and prevalence of life-history stages. Microstomes were then aseptically harvested by low speed centrifugation (200X g) of 500-ml volumes five minutes (using a Sorvall RC-5C centrifuge). The supernatant was vacuum aspirated in a sterile laminar flow-hood, the remaining cell pellets were resuspended in sterile 35 ppt salinity artificial seawater (ASW), and the samples were centrifuged again at 200X g for two minutes. This process was repeated until cells had been washed three times. After the final wash, half of the cells cultures were centrifuged at 1000X g to generate a single 5-ml cell pellet for poly (A) mRNA extraction. The other half of the cells culture was suspended in the prey-conditioned medium and placed in Costar ® 225 cm^2 culture flasks (Corning Inc., Corning, NY, USA #3001) with vent caps (10 flasks with 200 ml per flask). The cells were incubated for 2.5 h under standard growth conditions to induce microstome to macrostome transformation (= microstome-macrostome). A 1-ml aliquot was removed from each flask at the end of the incubation for determination of cell density and prevalence of life-history stages. Transforming cells were then

pelleted and washed as above to produce a single 5-ml cell pellet for poly (A) mRNA extraction.

Tomite-to-Microstome Transformation

To produce *M. avidus* tomites, 10 200-ml stock cultures of microstomes (i.e., log-growth cells at ~ 2.5 X 10^5 cells/ml) were sampled for determination of cell densities and prevalence of life-history stages and washed into 35 ppt ASW following methods above. After the final wash, half of the cells were centrifuged at 1000X g to generate a single 5-ml cell pellet for poly (A) mRNA extraction. The remainder of the cells were suspended in 15 ppt ASW and transferred to Costar ® 225 cm^2 culture flasks (10 flasks with 200 ml per flask). Flasks were incubated under standard growth conditions for 24 h, with a 1-ml aliquot removed from each flask at the end of the incubation for determination of cell density and prevalence of life-history stages

The resulting tomite cultures were induced to re-transform to microstomes (= tomite-microstome transforming cells) by transfer to sterile MA 1651 medium using centrifugation and washing procedures above. Washed tomites were distributed to Costar ® 225 cm^2 culture flasks (10 flasks with 200 ml per flask) and incubated for 2.5 h under standard conditions. Samples were taken from each flask for determination of cell density and prevalence of life-history stages at the end of the

incubation. Following incubation, cultures were pelleted and washed as above to produce a single 5-ml cell pellet for poly (A) mRNA extraction.

Isolation of Poly (A) mRNA from Life-History Stages of *Miamiensis avidus*.

Cell pellets from the microstome-macrostome and the tomite-microstome transformations were used to extract poly (A) mRNA for cDNA library synthesis. Poly (A) mRNA was isolated using Ambion's MicroPoly (A) Purist™ Small Scale mRNA Purification kit. Spectrophotometry ($OD_{260/280}$) and gel electrophoresis (1.2% formaldehyde-agarose) were used to assess the quantity and quality of the extracted poly (A) mRNA.

Subtraction Suppression Hybridization (SSH) of cDNA Libraries from Life-History Stages of *Miamiensis avidus*

Suppression subtraction hybridization (SSH) was conducted using poly (A) mRNA produced during the microstome-macrostome and the tomite-microstome transformation experiments. For each experiment, 1.0 μg poly (A) mRNA from microstomes and 1.0 μg poly (A) mRNA from the complimentary population of transforming *M. avidus* was amplified separately by PCR using the SMART PCR primers included in Clontech's Super SMART PCR cDNA synthesis kit (BD Biosciences, Palo Alto, CA, USA, #K1054-1). The thermocycler program was

initiated with 18 cycles of denaturing at 95 °C for 7 seconds, annealing at 65 °C for 20 seconds, and a final extension step at 72 °C for three minutes. The amplified single strand cDNAs were converted into double strand cDNA libraries by the SMART reverse transcriptase template-switching protocol included in Clontech's PCR-Select cDNA Subtraction Kit (BD Biosciences, Palo Alto, CA, USA, #K1804-1). Double stranded cDNA libraries were then digested using *Rsa* I restrictive enzyme prior to adaptor ligation.

After restrictive enzyme digestions, cDNA libraries for each transforming *M. avidus* population was divided into two "tester" fractions, one that was ligated with a forward adaptor (Adaptor 1 at the 5'end) and another that was ligated with a reverse adaptor (Adaptor 2R at the 3'end). Both adaptors were supplied with the Clontech PCR-Select cDNA Subtraction kit. Following adapter ligation, the two tester cDNAs were hybridized in the presence of excess non-ligated cDNA from the corresponding microstome culture. The resulting hybridized tester cDNAs were then hybridized with each other and subjected to three rounds of PCR amplification to produce a suppression subtraction hybridization library. The first two rounds of PCR used the Clontech's PCR-Select cDNA Subtraction Kit. The first PCR cycle incorporated a heat activation step at 94°C for 25 seconds, followed by 25 cycles of denaturing at 94°C for 10 seconds, annealing at 66°C for 30 seconds, and final extension at 72°C for 90 seconds. This was followed by nested PCR using 10 cycles of denaturing at 94 °C

for 10 seconds, annealing at 68 °C for 30 seconds, and final extension at 72 °C for 90 seconds. The final step was Mirror Orientation PCR Selection (MOS) following the procedures of Rebrikov et al., (2000) to reduce background cDNAs representing redundant, non-differentially expressed transcripts. Nested MOS amplification included 23 cycles of denaturing at 95 °C for 7 seconds, annealing at 62 °C for 20 seconds, and final extension at 72 °C for 120 seconds. A second set of suppression subtraction hybridization libraries representing microstome populations from the two experiments was produced in an analogous manner.

Dot-Blot Hybridization from SSH cDNA Clones

Purified SSH cDNAs from the microstome-macrostome and the tomite-microstome experiments were inserted into the pAL16 T/A electrocompetent cloning vector and transferred to *Escherichia coli*. Following insertion of SSH cDNAs, *E. coli* was cloned by plating onto Luria-Bertani (LB)/Ampicillin (75 ug/ml) selective agar. White colonies (positive insert) were randomly selected and transferred individually to separate wells of a 96-well plate. Ten 96-well plates were made for each transformation experiment, five from the starting microstome culture and five from the transforming population. Each well was supplemented with 100 µl LB/ Ampicillin (75 ug/ml) medium and 20 µl glycerol before being stored at -80°C as stock samples for differential screening.

Differential Screening of SSH cDNA Clones

Differential screening followed the strategy outlined in the PCR-Select Differential Screening Kit User Manual (BD Biosciences, Palo Alto, CA, USA, #637403). Plasmid inserts from individual stock colonies were PCR amplified in 96-well format, using Sp6 and T7 and forward/reverse vector primers (Promega, Madison, WI, USA #Q5011 and #Q5021). Amplification incorporated a heat activation step at 94 °C for 25 seconds, followed by 25 cycles of denaturing at 94 °C for 10 seconds, annealing at 66 °C for 30 seconds, and final extension at 72 °C for 90 seconds. Amplified inserts (~100 ng DNA) were arrayed in duplicate onto nylon membranes and hybridized with ^{32}P-labelled probes synthesized from the Differential Screening Kit. Dot-Blot arrays were hybridized at room temperature for 24-h and then used for overnight exposure of x-ray film. Clones were selected for further analysis based upon high positive hybridization signal to the forward probe and negative hybridization to the reverse probe.

Sequencing of Differentially Screened SSH cDNA Clones

Selected stock clones were individually transferred to fresh LB-Ampicillin medium and incubated overnight at 37 °C in sterile 96-well plates. Target cDNAs were removed from clones and purified using the Qiaprep-Spin Miniprep Kit (Qiagen, Valencia, CA, USA #27106). Purified cDNAs were sequenced in forward and reverse directions using ABI PRISM® BigDye® Terminator v3.1 Cycle Sequencing Kit (PE Applied Biosystems, Foster City, CA, USA), according to the manufacturer's protocol. Sequencher® Version 3.2 (Gene Codes Corporation, Ann Arbor, MI, USA) was used to construct and assemble expressed sequence tags (ESTs). The NCBI BlastX program provided by Genbank/EMBL was used to search for protein homologies of the ESTs.

Effects of the Proteasome Inhibitor *Lactacystin* on Microstome-Macrostome Transformation

The proteasome inhibitor *Lactacystin* (Cayman Chemical, Lansing, MI, USA, (#70980) was used to explore the potential role of *Ef-1*α in the microstome-macrostome transformation. Log-growth cultures of *M. avidus* ($1.7 \pm 0.53 \times 10^5$ cells/ml; n=3) with microstomes and macrostomes representing 95 $\pm$ 3.2 % and 5 $\pm$ 2.7% of the population, respectively (n=3), were washed into prey-conditioned medium as above and transferred to each of six Costar ® 225 cm^2 culture flasks. Three of the flasks received 40 μM *Lactacystin*, while three flasks without *Lactacystin*

served as controls. Flasks were incubated under standard growth conditions with 0.5 ml aliquots preserved with Bouin's fixative at T0 (immediately after transfer), 2.5 h, and 6 h for determination of cell abundance and life-history stages.

Effects of Cysteine Protease Inhibitors (*E64* and *Leupeptin*) on Tomite-Microstome Transformation

Log-growth cultures of *M. avidus* ($4.7 \pm 0.27 \times 10^4$ cells/ml; n=3) with microstomes and macrostomes representing 97 ± 1.9 % and 3 ± 0.8% of the population, respectively (n=3*)* were transformed into tomites using methods above and distributed to nine Costar ® 225 cm^2 culture flasks. Three of the flasks received 10 μM *E64*, three received 10 μM *Leupeptin*, and three control flasks received no additions. Flasks were incubated under standard growth conditions, with 0.5 ml aliquots preserved with Bouin's fixative at T0, 2.5 h, and 6 h for determination of cell abundance and life-history stages.

Cytological Staining, Cell Counts, and Assessment of Life-History Stages

Bouin's preserved samples were processed by Quantitative Protargol Staining (QPS) following the protocol of Montagnes and Lynn (1987), with ciliate abundance determined at 600-1250X by counting cells present in five arbitrarily selected fields of

view (~300 cells/field). Cells present in each field were categorized by life-history stage following criteria of Gomez-Saladin and Small (1993a,b).

Results

Up-Regulation of Genes During Microstome-to-Macrostome Transformation

An experiment was initiated using log-growth cultures of *Miamiensis avidus* Strain MA/2 ($2.5 \pm 0.37 \times 10^5$ cells/ml) that consisted primarily of microstomes, with macrostomes representing only $2 \pm 1.1\%$ (n = 20) of the populations. Microstomes (Fig 3-1a) had a reduced oral dikinetid C segment, lacked a cytopharyngeal pouch, and had small food vacuoles. Macrostomes (Fig 3-1b) typically had an oral dikinetid B segment that extended approximately one-half the length of the cell, a large cytopharyngeal pouch, and large food vacuoles. Treatment of log-growth cultures with prey-conditioned medium for 2.5 h, yielded microstome-to-macrostome (= microstome-macrostome) transforming populations having $74 \pm 4.2\%$ (n = 10) microstomes and $26 \pm 3.9\%$ (n = 10) macrostomes. Poly (A) mRNA extraction, yielded 11.2 μg and 9.6 μg of nucleic acid for microstomes (= log-growth cells) and microstome-macrostome transforming cultures, respectively.

Subtracted cDNA libraries consisting of 480 clones for microstome cultures and 480 clones for microstome-macrostome transforming cells contained unedited sequences ranging in size from 0.3 to 2.0 kilobases. Of the 480 clones from *M. avidus* microstomes, 117 represented up-regulated sequences not detected in the microstome-

macrostome transforming populations. By comparison, 125 of the ESTs from microstome-macrostome transforming cells were not detected in microstomes.

Twelve up-regulated genes were identified using the 117 ESTs from microstomes, eight of which were homologous to genes previously isolated from eukaryotes (Table 3-1). The remaining four genes did not align to sequences provided in Genbank. The eight identified genes sorted as four related to metabolic processes (asparagine synthetase, fructose bisphosphate aldolase, DNA kinase, and ATP synthase), three associated with ribosomal assembly (Ribosome 10, 18, and 32 genes), and one having a domain similar to a domain in the elongation-growth-factor gene (see Figure 3-2 for representative plates of genes differentially expressed by microstomes).

Twenty up-regulated genes were identified using the 125 ESTs from microstome-macrostome transforming *M. avidus*, 17 of which were homologous to genes previously isolated from eukaryotes (Table 3-2), while three failed to align with previously reported gene sequences. Three of the genes were associated with ribosomal assembly (ribosomal L2, L5, 40S genes), three coded for tubulin (alpha, beta, and beta-2), two were linked with metabolism (cytochrome P450 and an amidase family genes), one was a protein kinase, and one coded for a protein associated with the plasma membrane. The remaining seven genes have been implicated in cell-cycle control and transformation processes in other eukaryotes. Those genes were

elongation factor-1 alpha (*Ef-1*α), Constans, Constans-like & TOC1 (CCT) transcription factor, heat shock protein 70 (*Hsp70*), a WD40-16 repeat protein, a disulfide isomerase, step II splicing factor (*Slu7*), U1 and zinc finger domain (see Figure 3-3 for representative plates of differentially expressed gene in microstome-macrostome transforming cells).

Up-Regulation of Genes During Tomite-to-Microstome Transformation

A second experiment was initiated using 10 log-growth cultures (2.5 X 10^5 cells/ml) consisting of microstomes (96 $\pm$ 2.1%; n = 10) and macrostomes (4 $\pm$ 1.9%; n = 10). After 24-h treatment of log-growth cultures with sterile 15 ppt ASW, the populations contained 3 $\pm$ 1.8% microstomes, 97 $\pm$ 1.2% tomites, and no detectable macrostomes (n = 10). Tomites were typically small fast swimming cells that lacked oral structures and food vacuoles (Figure 3-1C). Cell density of "tomite-transformed" cultures averaged 4.7 $\pm$ 0.31 X 10^5 cells/ml, indicating cell division of microstomes following transfer to 15 ppt ASW. Treatment of the tomite-transformed cultures with MA 1651 nutrient medium for 2.5 h yielded tomite-to-microstome (= tomite-microstome) transforming populations having 32 $\pm$ 3.8 % tomites and 68 $\pm$ 4.7% microstomes, with cell density averaging 3.9 $\pm$ 0.29 X 10^5 cells/ml (n = 10). Poly (A) mRNA extraction yielded 12.2 µg and 8.2 µg of nucleic acid for microstome and tomite-microstome transforming populations, respectively.

Subtracted cDNA libraries consisting of 480 clones for microstomes (i.e., log-growth) cultures and 480 clones for tomite-microstome transforming *M. avidus* contained sequences ranging in size from 0.3 to 1.8 kilobases. Of the 480 clones from microstome cultures, 150 represented up-regulated genes that were not detected in the tomite-microstome transforming populations. Similarly, 150 of the ESTs from tomite-to-microstome-transforming *M. avidus* were not detected in microstomes.

Six up-regulated genes were identified using the 150 microstome ESTs, all of which were homologous to genes previously isolated from other ciliates (Table 3-4). The six identified genes sorted as four related to metabolic processes (cytochrome C1, glucose-6-phosphate isomerase, pyrophosphatase, and fructose-bisphosphate aldolse), one associated with DNA transcription (histone 3), and one coded for beta tubulin. See Figure 3-4 for representative plates of differentially expressed sequence in microstome populations.

Seventeen up-regulated genes were identified using the 150 ESTs from tomite-microstome transforming *M. avidus*, all of which were homologous to genes previously isolated from eukaryotes (Table 3-4). Of those 17 genes, six were related to metabolic processes (Na/K antiporter P-type ATPase, lecithin-cholesterol acyltransferase, malate dehydrogenase, acetyl-coenzyme acyltransferase I, citrase synthase I, and cytochrome B5), three were related to DNA translation/transcription (von Wildebrand factor type-A, ubiquitin carboxyl-terminal hydroxylase, and

elongation factor 2), one was related to ribosomal assembly (ribosomal L3), and two sorted as genes isolated from other ciliates whose functions lack formal description in Genbank (hypothetical *Paramecium tetraurelia* and hypothetical *Tetrahymena thermophila* genes). Additionally, two genes aligned with a cysteine proteases lacking formal description (papain-family cysteine protease and *XCP1* cysteine protease), two aligned with described cysteine proteases (cathepsin B and cathepsin L), and one aligned with a cysteine protease inhibitor (cystatin-1). Figure 3.5 show plates depicting differential expression of the genes for cathepsin B, cathepsin L, *XCP1*, and cystatin-1, all of which have been associated with cell transformation processes in pathogenic protists. The amino acid sequence deduced from the EST library confirmed the presence cysteine residues and active sites for cathepsin B and cathepsin L (Figure 3-6).

Effects of the Proteasome Inhibitor *Lactacystin* on Microstome-Macrostome Transformation

Of the differentially expressed genes detected in microstome-macrostome transforming *Miamiensis avidus*, elongation factor-1 alpha (*Ef-1*α) appeared most likely linked with morphogenetic events, as its transcription product stabilizes the eukaryotic proteasome associated with many cell transformation processes. To explore the potential role of *Ef-1*α in microstome-macrostome transformation, an experiment was conducted using the proteasome inhibitor *Lactacystin*.

Immediately after transferring log-growth *M. avidus* to prey-conditioned medium containing 40 μM *Lactacystin*, cell density averaged 9.6 $\pm$ 0.31 X 10^4 cells/ml (n=3), with microstomes and macrostomes representing 96 $\pm$ 4.8% and 4 $\pm$ 3.8% of the population, respectively (n=3). *M. avidus* abundance and proportional representation of microstomes was comparable in controls (Figure 3-7). While cell densities remained unchanged in treatments and controls throughout the experiment (data not shown), the prevalence of macrostomes varied with time (Figure 3-7). Neither the *Lactacystin*-treated cultures nor controls showed a change in the occurrence of life-history stages after 2.5 h ($p = 0.08$). Six hours after treatment the percent of cells as macrostomes had increased in all cultures, with mean values for *Lactacystin*-treated cultures (32 ± 3.5%) being significantly lower ($p=0.05$) than controls (62 ± 2.5%). In addition to microstomes and macrostomes, cultures treated with *Lactacystin* for 6 h contained a small number of individuals with aberrant morphology (Figure 3-1d). Those specimens had an oral dikinetid segment B that was that composed of two fragments, suggesting incomplete oral replacement during macrostome formation.

Effects of the Cysteine Protease Inhibitors, *E64* and *Leupeptin* on Tomite-Microstome Transformation

Two genes differentially expressed in tomite-microstome transforming *Miamiensis avidus* have been affiliated previously with cell transformation processes

in ciliates. Thus, experiments were conducted to examine the transition from tomites-to-microstomes when the expression the cysteine proteases was blocked using either *E64* or *Leupeptin*.

Immediately after transferring tomite-transformed *M. avidus* to *E64* or *Leupeptin* (T0), cell density averaged 9.6 $\pm$ 0.52 X 10^4 cells/ml (n=3), with tomites and microstomes representing 93 $\pm$ 3.8% and 7 $\pm$ 1.8% of the population, respectively (n=3). *M. avidus* abundance and proportional representation of microstomes was comparable in controls (Figure 3-8). While cell density remained unchanged in treatments and controls throughout the experiment (data not shown), the transformation of tomites to microstomes was inhibited by exposure to *E64* and *Leupeptin* (Fig. 3-8). After 2.5 h, microstomes represented 67 $\pm$ 4.6% of the cells in control cultures. Values for *E64* and Leupetin treatments were significantly lower ($p = 0.05$), averaging 32 ± 4.1% and 31 ± 5.6%, respectively. Inhibition of tomite-microstome transformation was more evident following 6-h incubation, with prevalence of microstomes averaging 89 $\pm$ 3.1 %, 37 ± 3.0%, 33 ± 1.7% for controls, *E64* treatments, and Leupetin treatments, respectively (Fig. 3-8).

Table 3-1. Sequence Length, E-values, and Blast Hits for Up-Regulated Genes Identified from Axenic Cultures of *Miamiensis avidus* Microstomes prior to Microstome-Macrostome Transformation.

Table 3-1. Sequence Length, E-values, and Blast Hits for Up-Regulated Genes Identified from Axenic Cultures of *Miamiensis avidus* Microstomes prior to Microstome-Macrostome Transformation.

Name	Length	Gene Information	*E*-Value	Organism
2BN2DO4	457bps	Gene containing EGF-Like Domain	1.00E-13	*Tetrahymena thermophila*
Contig 8	333bps	Ribosomal L32 gene	2.00E-24	*Tetrahymena thermophila*
2BN1HO6	444bps	Asparagine Synthetase	1.00E-28	*Danio rario*
2BN3A11	876bps	Ribosomal L10 gene	2.00E-46	*Tetrahymena thermophila*
2BN4C02	691bps	DnaK gene	3.00E-50	*Tetrahymena thermophila*
Contig 7	659bps	Ribosomal L18 gene	6.00E-55	*Tetrahymena thermophila*
Contig 6	905bps	Fructose Bisphosphate Aldolase	3.00E-88	*Tetrahymena thermophila*
Contig 3	788bps	ATP Synthase Subunit Beta	2.00E-98	*Paramecium tetraurelia*
Contig 1	1067bps	Unknown		
Contig 2	880bps	Unknown		
Contig 4	776bps	Unknown		
Contig 5	827bps	Unknown		

Table 3-2. Sequence Length, E-values, and Blast Hits for Up-Regulated Genes Identified from Axenic Cultures of Microstome-Macrostome Transforming *Miamiensis avidus.*

Table 3-2. Sequence Length, E-values, and Blast Hits for Up-Regulated Genes Identified from Axenic Cultures of Microstome-Macrostome Transforming *Miamiensis avidus.*

Name	Length	Gene Information	*E*-Value	Organism
Contig 5	832bps	Protein Kinase-Like gene	0.005	*Entamoeba histolytica*
Contig 3	940bps	Amidase Family gene	2.00E-05	*Tetrahymena thermophila*
2AN3H08	754bps	U1 Zinc Finger gene	3.00E-09	*Trichomonas vaginalis*
2AN4A02	455bps	Variant Specific Surface gene	1.00E-10	*Giardia intestinalis*
Contig 2	1510bps	Beta Tubulin-1	1.00E-10	*Paramecium tetraurelia*
2AN1E07	1281bps	Alpha Tubulin	1.00E-11	*Mesenchtraeus solifugus*
2AN5F07	1241bps	CCT gene	2.00E-14	*Tetrahymena thermophila*
2AN1F10	1311bps	Cytochrome P450	2.00E-19	*Tetrahymena thermophila*
Contig 7	1379bps	Disulfide Isomerase Domain gene	3.00E-20	*Tetrahymena thermophila*
2AN3F04	639bps	Step II Splicing Factor-*Slu7*	1.00E-22	*Paramecium tetraurelia*
2AN2D01	897bps	Ribosomal L2 gene	1.00E-23	*Tetrahymena thermophila*
2AN2H02	837bps	Ribosomal L5 gene	4.00E-41	*Tetrahymena thermophila*
2AN4D12	627bps	Beta Tubulin-2	2.00E-46	*Paramecium tetraurelia*
2AN3H12	873bps	40S Ribosomal gene	3.00E-56	*Trypanosoma cruzi*
2AN3F06	1280bps	WD40-16 Repeat gene	4.00E-60	*Homo sapiens*
2AN2D01	603bps	Elongation Factor 1 alpha gene	2.00E-66	*Stylonychia lemnae*
2AN2A02	1236bps	Heat Shock Protein 70 gene	3.00E-77	*Tetrahymena thermophila*
Contig 1	1326bps	Unknown		
Contig 4	948bps	Unknown		
Contig 6	561bps	Unknown		

Table 3-3. Sequence Length, E-values, and Blast Hits for Up-Regulated Genes Identified from Axenic Cultures of *Miamiensis avidus* Microstomes prior to Tomite-Microstome Transformation.

Table 3-3. Sequence Length, E-values, and Blast Hits for Up-Regulated Genes Identified from Axenic Cultures of *Miamiensis avidus* Microstomes prior to Tomite-Microstome Transformation.

Name	Length	Gene Information	*E*-Value	Organism
1BN1G06	1124bps	Histone 3 gene	3.00E-49	*Tetrahymena thermophila*
1BN3G04	757bps	Cytochrome C1	1.00E-73	*Tetrahymena thermophila*
1BN2E12	893bps	Glucose-6-Phostphate Isomerase	2.00E-82	*Tetrahymena thermophila*
1BN3G06	1201bps	Pyrophosphatase	1.00E-105	*Tetrahymena thermophila*
Contig3	647bps	Fructose-Biphosphate Adolase	1.00E-112	*Tetrahymena thermophila*
1BN4C08	934bps	Tubulin Beta-1 chain	1.00E-134	*Paramecium tetraurelia*

Table 3-4. Sequence Length, E-values, and Blast Hits for Up-Regulated Genes Identified from Axenic Cultures of Tomite-Microstome Transforming *Miamiensis avidus.*

Table 3-4. Sequence Length, E-values, and Blast Hits for Up-Regulated Genes Identified from Axenic Cultures of Tomite-Microstome Transforming *Miamiensis avidus.*

Name	Length	Gene Information	*E*-Value	Organism
Contig10	817bps	Papain-Family Cysteine Protease	3.00E-07	*Paramecium tetraurelia*
1AN2H01	1251bps	Cystatin-1 Cysteine Proteinase Inhibitor	1.00E-07	*Solanum tuberosum*
Contig 9	1447bps	Hypothetical *Paramecium tetraurelia* gene	6.00E-11	*Paramecium tetraurelia*
1AN3D06	887bps	Na/K Antiporter P-type ATPase	5.00E-11	*Tetrahymena thermophila*
1AN1H04	843bps	Hypothetical *Tetrahymena thermophila* gene	4.00E-11	*Tetrahymena thermophila*
Contig16	382bps	*XCP1* Cysteine Protease	3.00E-21	*Arabidopsis thaliana*
Contig8	593bps	von Wildebrand Factor Type A Domain gene	2.00E-31	*Tetrahymena thermophila*
1AN3F10	714bps	Ubiquitin Carboxyl-Terminal Hydroxylase gene	5.00E-32	*Tetrahymena thermophila*
1AN1B08	1231bps	Lecithin-Cholesterol Acyltransferase	8.00E-39	*Tetrahymena thermophila*
1AN2A10	1165bps	Cathespin L Cysteine Protease	2.00E-43	*Uronema marinum*
1AN1F01	606bps	Malate Dehydrogenase	7.00E-57	*Tetrahymena thermophila*
1AN2C04	549bps	Elongation Factor 2	5.00E-65	*Tetrahymena thermophila*
1AN4G03	769bps	Ribosomal Protein L3	9.00E-68	*Tetrahymena thermophila*
1AN1G03	1201bps	Cathespin B Cysteine Protease	1.00E-81	*Uronema marinum*
Contig7	994bps	Acetyl-Coenzyme Acyltransferase I	2.00E-88	*Paramecium tetraurelia*
Contig1	707bps	Citrase Synthase I	4.00E-89	*Tetrahymena thermophila*
Contig5	1251bps	Cytochrome B5	3.00E-95	*Ostreococcus tauri*
1AN5G05	498bps	Unknown (Ferredoxin Binding Region)		
Contig 6	1378bps	Unknown (EGF-2-like domain)		
Contig24	924bps	Unknown		
1AN1G03	153bps	Unknown		

Figure 3-1. Life-history stages of *Miamiensis avidus* Strain Ma/2 following Protargol silver impregnation. (a) microstome, (b) macrostome, (c) tomite with oral region (arrow) lacking ciliature, (d) aberrant macrostome characteristic of *Lactacystin* treated cells; note the fragmented ODkB indicative of incomplete oral replacement. ODkA, ODkB, and ODkC = oral dikinetid segments A, B, and C, respectively. Scale bars = 5 μm.

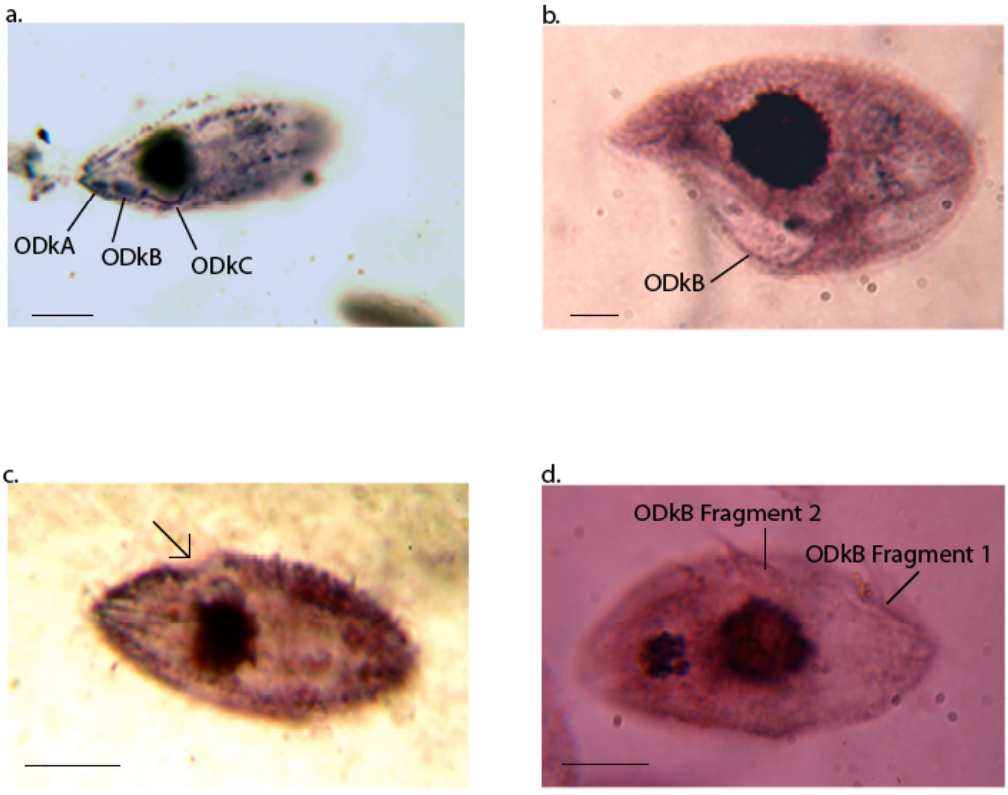
a.
ODkA
ODkB
ODkC
b.
ODkB
c.
d.
ODkB Fragment 2
ODkB Fragment 1

Figure 3-2. Dot-blot plates for suppression subtraction hybridization of *Miamiensis avidus*. (a) Forward (= tester) and (b) reverse (= driver) probes for three sets of 96 cDNA clones from microstome cultures prior to microstome-macrostome transformation. Clones were differentially screened with a forward probe for microstomes (1a-3a) and a reverse probe for microstome-macrostome transforming cells (1b-3b). Red circles indicate positive hits with forward probe, with blue circles showing corresponding negative hits with the reverse probe. Clones G2 (1a and 1b), E12 (2a and 2b), H11 (2a and 2b), and E9 (3a and 3b) expressed genes for fructose bisphosphate aldolase, asparagine synthetase, ATP synthase subunit beta, and ribosomal L32, respectively.

non-transformed microstome forward probe

1a.

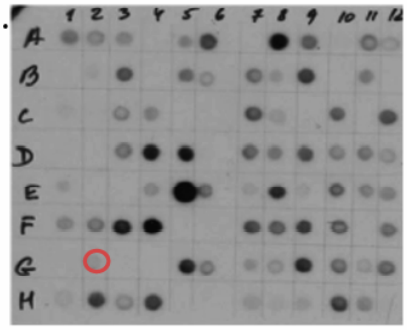

microstome-macrostome transforming reverse probe

1b.

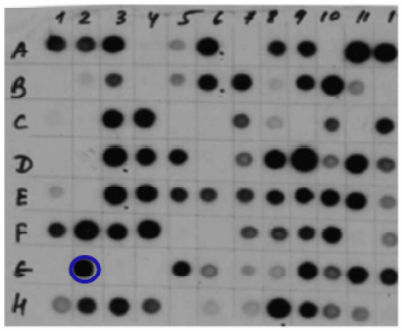

2a.

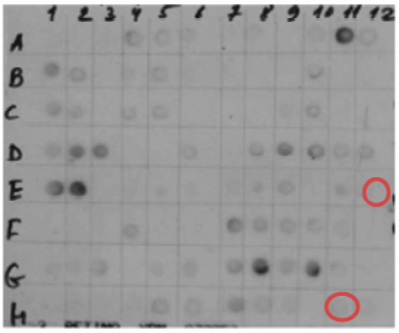

2b.

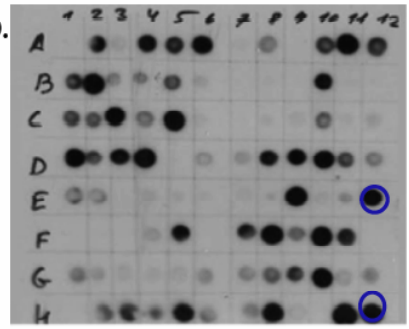

3a.

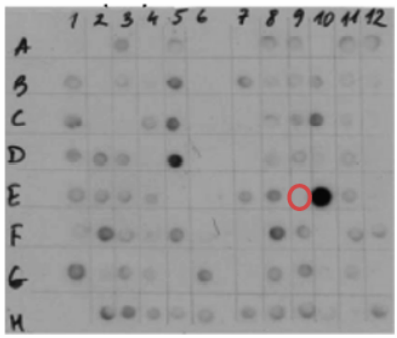

3b.

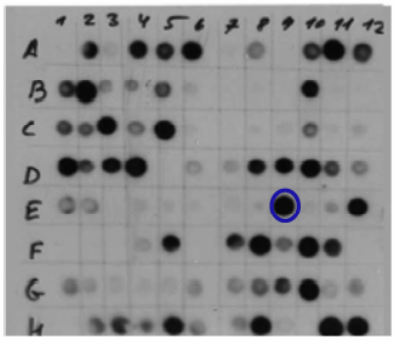

Figure 3-3. Dot-blot plates for suppression subtraction hybridization of *Miamiensis avidus*. (a) Forward (= tester) and (b) reverse (= driver) probes for three sets of 96 cDNA clones from microstome-macrostome transforming cultures. Clones were differentially screened with forward probe for microstome-macrostome transforming (1a-3a) and a reverse probe for microstomes (1b-3b). Red circles indicate positive hits with forward probe, with corresponding negative hits with the reverse probe indicated by blue circles. Clones A2 (1a and 1b), D1 (1a and 1b), F4 (2a and 2b), F6 (2a and 2b), H5 (2a and 2b), and F7 (3a and 3b) expressed heat shock protein 70, elongation factor 1-alpha, step II splicing factor (*Slu7*), WD40 16-repeat, U1 zinc finger, CCT (Constans, Constans-like & TOC1) transcription factor, respectively.

microstome-macrostome
transforming forward probe

non-transformed microstome reverse probe

1a.

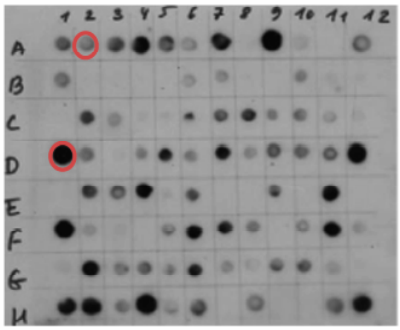

1b.

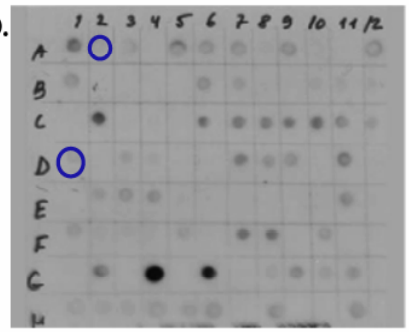

2a.

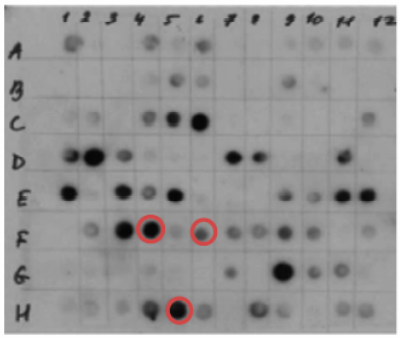

2b.

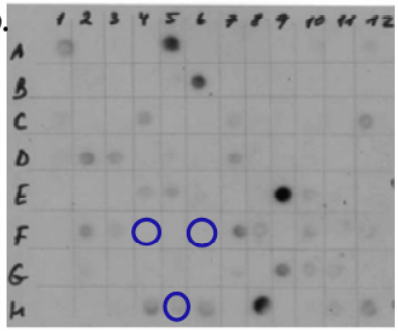

3a.

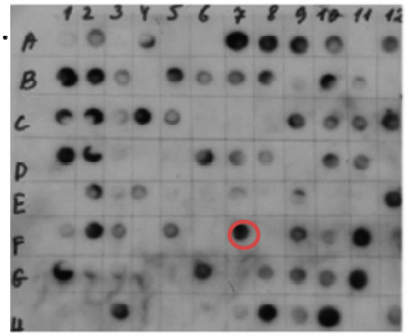

3b.

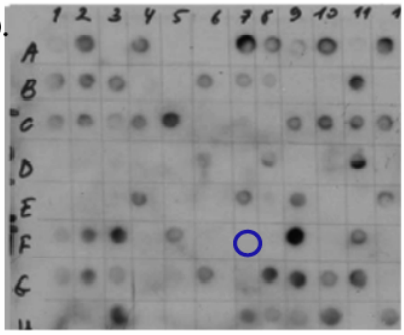

Figure 3-4. Dot-blot plates for suppression subtraction hybridization of *Miamiensis avidus*. (a) Forward (= tester) and (b) reverse (= driver) probes for three sets of 96 cDNA clones from microstome cultures prior to tomite-microstome transformation. Clones were differentially screened with tomite-microstome transforming reverse probe (1a-3a) and a forward probe for microstomes (1b-3b). Red circles indicate positive hits with reverse probe and correspond to blue circles over negative hits with the forward probe. Clone G2 (1a and 1b), G12 (1a and 1B), D5 (2a and 2b), and H9 (2a and 2b) expressed genes glucose-6-phostphate isomerase, beta tubulin, pyrophosphatase, and cytochrome C, respectively.

tomite-microstome
transforming reverse probe

non-transformed microstome forward probe

1a.

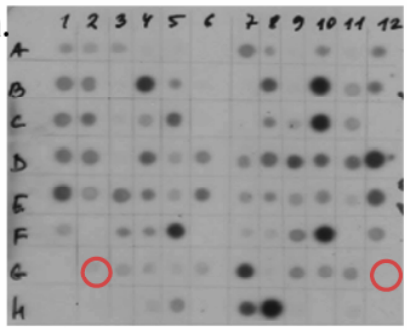

1b.

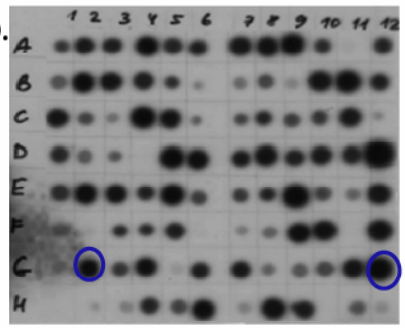

2a.

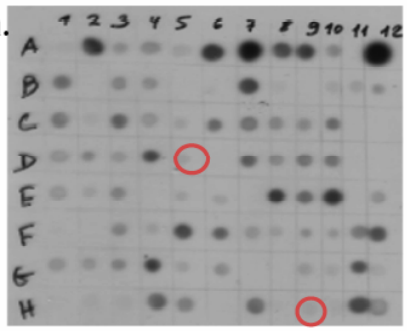

2b.

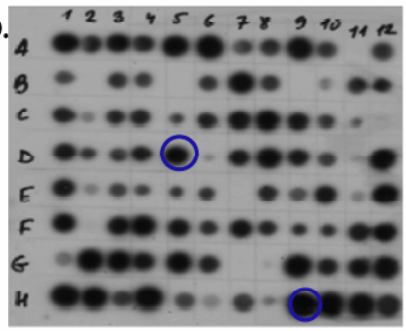

Figure 3-5. Dot-blot plates for suppression subtraction hybridization of *Miamiensis avidus*. (a) Forward (= tester) and (b) reverse (= driver) probes for three sets of 96 cDNA clones from tomite-microstome transforming cultures. Clones were differentially screened with forward probes for tomite-microstome transforming cells (1a-3a) and a reverse probe for microstomes (1b-3b). Red circles indicate positive hits with forward probe, with corresponding negative hits with the reverse probe indicated by blue circles. Clones C2 (1a and 1b), G3 (1a and 1b), A10 (2a and 2b), and B3 (2a and 2b) expressed genes for *XCP1* cysteine protease, cathepsin B cysteine protease, cathepsin L cysteine protease and cystatin-1 cysteine protease inhibitor, respectively.

tomite-microstome
transforming forward probe

1a.

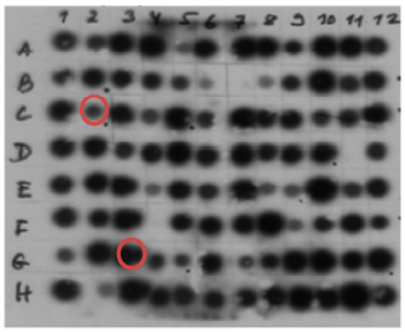

non-transformed microstome reverse probe

1b.

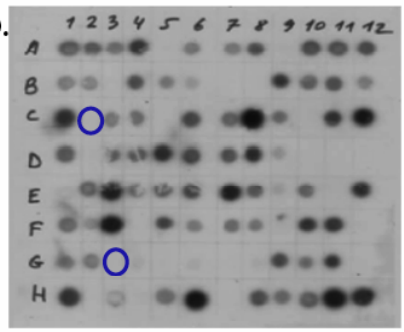

2a.

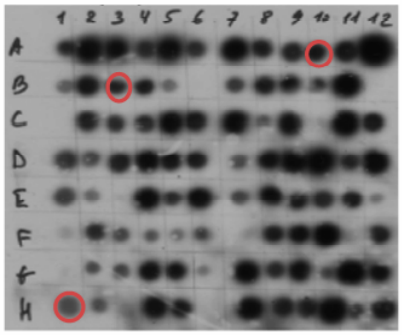

2b.

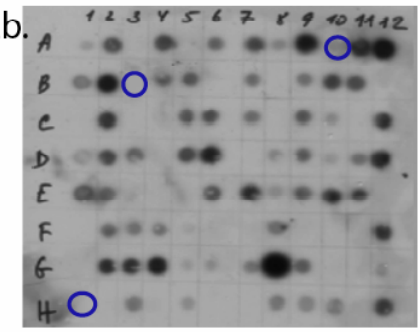

Figure 3-6. Amino acid sequences from ESTs isolated from tomite-microstome transforming *Miamiensis avidus*. (a) catalytic region for cathepsin-B gene. (b) cathepsin-L gene. Sequences are shown from N-to-C terminus. Catalytic sites are underlined and the characteristic conserved cysteine residues are highlighted in yellow.

a.

MGFHLRPTLLSPPSWIEVLKNVAVWPLFGPWIQQAPPVELPLSLRRPDPLDVRAEYAGKLIHEYSLNIL
DRQDYGATRTLHEILKIISLKKTFSPRRIDSRTQWPNCQSIKEIRDQSNCGSCWAFSAVEAFSDRICIQ
SGQQSQTRISSANLLSCCRGAFACGDGCDGGYISGAWRYFVKTGVVTGNLYGEDQYCQPYPFEPCSHHV
TGKYKPCGDGPEEKTPACSHECNSDYKGAAYNEDKHFAGSAYSIPRNVKNIQQELFTNGPVSASFTVFE
DFLTYKTGVYQHKTGRVLGGHAIKIIGYGVENGTPYWTVVNSWNETWGDNGTKILRGVNECGIESNIQA
GKVGSNARL

b.

MFASQDSSAPVLKMAMSQESKIYQQYMEWKQVYGSFTNGDEDAQKFSVFRENVLKIDQENAMDQGFTLG
VNQFAAMTTEEFKAISLGLLESKDNYQGEFDDMKVEEVVLPTDNLPKAVDWRQKGAVGPISQQQGDCGGC
WAFGSVAALEGLQKINEDKLIPLSQQQLLNCVGPIPGKPQTGGCGGQNSYFAFYYTQKHGIESAQDYPF
INQHSVKTLGKCEYDSSKVVFQNKGLGAVKDNNPDQLRARVNVQPTAVIINGSSFYMQFYKTGILKTPK
CTSAAT

Figure 3-7. Effects of the Proteasome Inhibitor *Lactacystin* on Microstome-Macrostome Transformation in *Miamiensis avidus*. Blue and red graphs represent percent microstomes and macrostomes respectively, in treatments and controls at (a) 0, (b) 2.5, and (c) 6 h after transfer of cells to prey-conditioned medium. Treatments contained 40 μm *Lactacystin.* Error bars represent one standard deviation (n=3).

a.

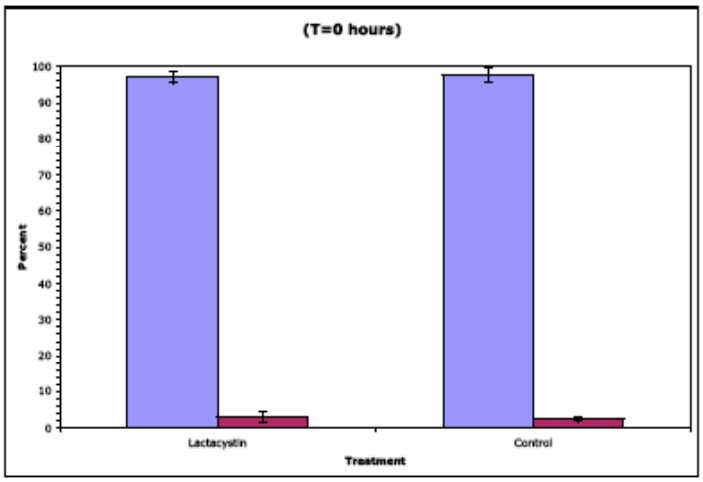
(T=0 hours)
Percent
100
90
80
70
60
50
40
30
20
10
0
Lactacystin
Control
Treatment

b.

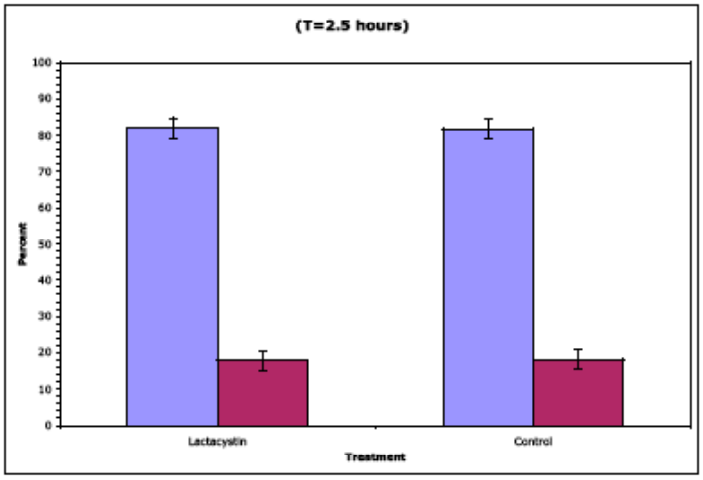
(T=2.5 hours)
Percent
100
90
80
70
60
50
40
30
20
10
0
Lactacystin
Control
Treatment

c.

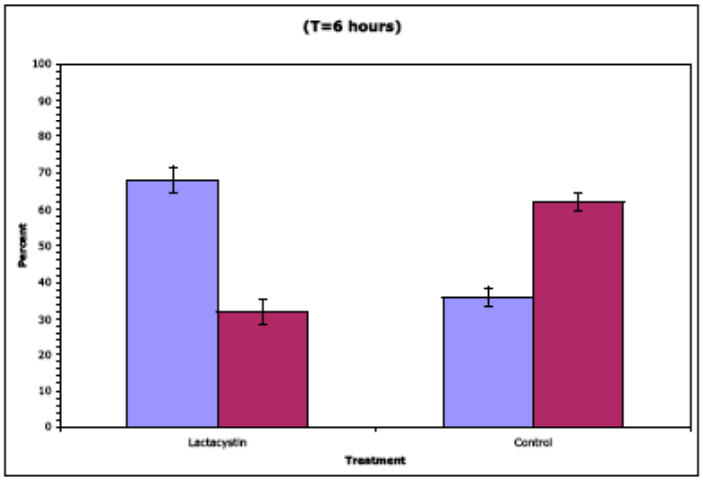
(T=6 hours)
Percent
100
90
80
70
60
50
40
30
20
10
0
Lactacystin
Control
Treatment

Figure 3-8. Effects of Cysteine Protease Inhibitors, *E64* and *Leupeptin*, on Tomite-Microstome Transformation in *Miamiensis avidus*. Blue and red graphs represent percent tomites and microstomes respectively, in treatments and controls at (a) 0, (b) 2.5, and (c) 6 hours following transferred of tomite-transformed cultures to MA 1651. Treatments contained either 10 μM *E64* or 10 μM *Leupeptin*. Error bars represent one standard deviation (n=3).

a.

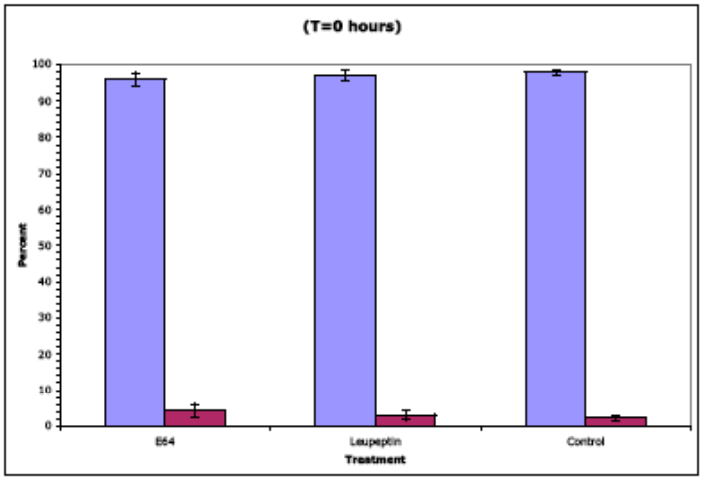
(T=0 hours)
Percent
100
90
80
70
60
50
40
30
20
10
0
E64
Leupeptin
Control
Treatment

b.

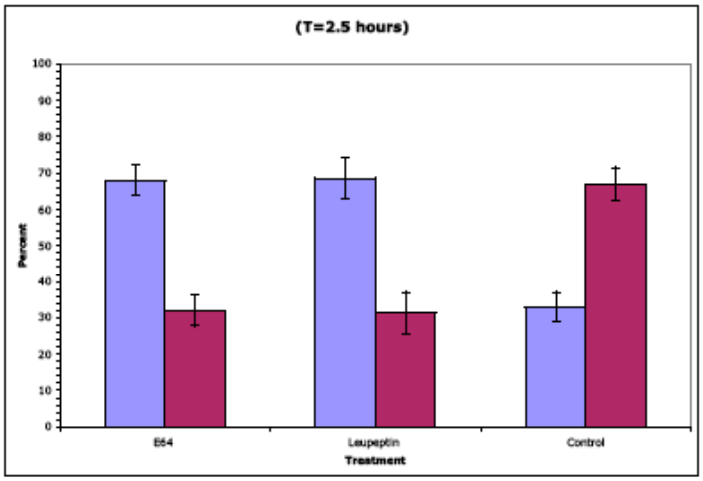
(T=2.5 hours)
Percent
100
90
80
70
60
50
40
30
20
10
0
E64
Leupeptin
Control
Treatment

c.

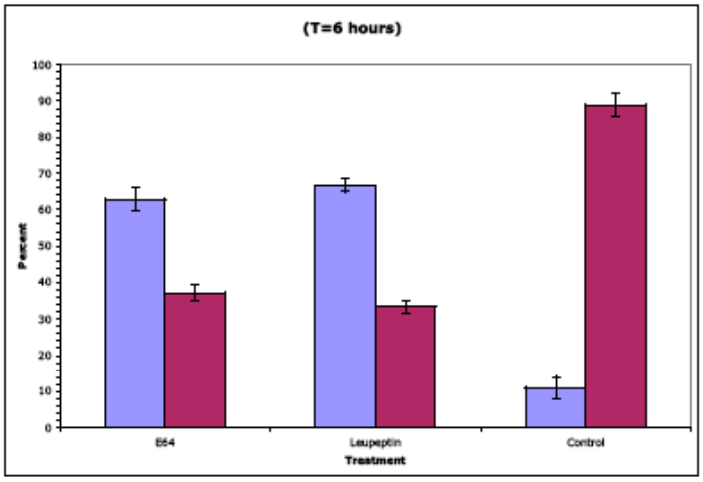
(T=6 hours)
Percent
100
90
80
70
60
50
40
30
20
10
0
E64
Leupeptin
Control
Treatment

Discussion

In *M. avidus*, extensive rearrangement and assembly of fibers and microtubular structures associated with ciliary bases occurs during transformation from microstome-to-macrostome and tomite-to-microstome (Gomez-Saladin and Small 1993a-c). During microstome-to-macrostome transformation, the parental microstome oral apparatus is completely dedifferentiated, and new macrostome oral structures are formed from an anlage derived from parental oral structures (Gomez-Saladin and Small 1993b and c). This process occurs in a regulated manner as the anlage organizes into six columns of pro-kinetids (Gomez-Saladin and Small 1993b and c). During microstomatogenesis, tomites are returned to nutrient medium, the oral apparatus redifferentiates to the microstome oral structures with clearly defined oral polykiniteds (Gomez-Saladin and Small 1993c). Until now, only cell signaling, signal interpretation, and morphological mechanisms of cortical changes have been described. Expression of genes relative to morphology transformations during life history stages of *M. avidus* was previously unknown. Using a suppression subtraction hybridization procedure seven genes previously implicated in cell-cycle control and transformation processes in eukaryotes were identified from *M. avidus* populations undergoing microstome-to-macrostome transformation. Additionally, two cysteine proteases and a cysteine protease inhibitor previously implicated in metamorphic processes in parasitic protists were isolated from *M. avidus* populations transitioning from tomites to microstomes.

Genes Identified from *M. avidus* Microstome-to-Macrostome Transformation

Elongation factor-1 alpha (*Ef-1*α), an essential component of the eukaryotic translational apparatus, was isolated from the microstome-to-macrostome transforming population. The 20S and 26S proteasomes are responsible for trafficking of newly synthesized proteins and recycling of proteins tagged for degradation. *Ef-1*α binds aminoacyl-transfer RNAs directly to the proteasome prior to protein synthesis. When *Ef-1*α is not bound to the proteasome, transcription/translation halts. In this way, the *Ef-1*α regulates genes expressed during the cell cycle (Tokumoto et al., 2003; Tuhackova et al., 1985). Uncoupling the *Ef-1*α–proteasome complex causes the accumulation of un-recycled proteins and halts many cell cycle mechanisms (Tokumoto et al., 2003).

During macrostome-microstome transformation in *M. avidus*, proteins associated with feeding structures are recycled as the parental microstome oral apparatus is resorbed and a new marcrostome oral apparatus is assembled. The *Ef-1*α –proteasome complex may facilitate recycling of dedifferentiated microstome ciliary structures. The inhibition of microstome-to-macrostome transformation by *Lactacystin* suggests that the *Ef-1*α –proteasome complex may be responsible for recycling parental oral ciliature and kinetids. The subsequent build up of un-recycled proteins during proteasome inhibition may have interfered with the synthesis of new structures, causing the transformation process to halt. Additionally, Shiina et. al. (1994) demonstrated that the expression of *Ef-1*α was involved in microtubules

disassembly and reorganiztion during *Xenopus sp*. cell cycle (Shiina et al., 1994). Through alternative mechanisms, *Ef-1*α may directly regulate organization of microstome and macrostome transformation by regulating the stability of microtubule based oral structures.

The Constans, Constans-like & TOC1 (CCT) transcription factor expressed during microstome-to-macrostome transformation was previously described from flowering multicellular plants such as *Arabidopsis ssp*. and single celled photosynthetic organisms such as *Chlamydomonas reinhardii* (Griffiths et al., 2003; and Strayer et al., 2000). The CCT transcription factor regulates the photoperiod pathway of the flowering cycle of monocot and dicot plants (Griffiths et al., 2003). An induced mutation to the TOC1 domain prevented expression of the CCT transcription factor and decreased the circadian period in light-grown *Arabidopsis* plants (Strayer et al., 2000). Strayer et al., (2000) also isolated and characterized the CCT sensor and the response receiver domain found on several plant clock genes that promotes growth of the flower (Strayer et al., 2000). In a similar manner, the *M. avidus* CCT transcription factor may interact with sensor and response receiver domain. This interaction may promote the synthesis of other genes that initiate the mechanism of dedifferentiation of the microstome oral kinetids and/or subsequent reconfiguration of the macrostome oral structures at the end of macrostome formation. This is an especially attractive theory, considering that in the CCT transcription factor directs structural changes in other organisms such as flowering plants.

Two apoptosis related genes, heat shock protein 70 (*Hsp70*) and the WD Repeat Under-Expressed in Humans (WDRPUH) gene were expressed during macrostome transformation. *Hsp70* assists the folding of newly synthesized polypeptides, assembles multiprotein complexes, transports proteins across cellular membranes, and targets proteins for subsequent degradation (McKay 1993). A higher concentration of *Hsp70* prevents activation of the caspase-dependent apoptosis pathway and alters apoptosis protease activating factor-1 (AIF) in cancerous cells (Nylandsted et al., 2004, Gyrd-Hansen et al., 2004; Ravagnan et al., 2001; Rohde et al., 2005). Rohde et al., (2005) demonstrated that over-expression of *Hsp70* in cancerous cells resulted in change of cell morphologies and accelerated cell proliferation (Rhode et al., 2007). Knock out experiments of human hepatocellular cancer cells demonstrated that the WDRPUH gene also decreased cell viability, by limiting cell growth and inducing apoptosis (Silva et al., 2005). WDRPUH interacts with *Hsp70* through mechanisms that remain unclear, to increase proliferation and prevent apoptosis of cancerous cells (Silva et al., 2005). A mutation WD repeat gene, *Pro11*, prevented the synthesis of fruiting bodies generated during the sexual life cycle of filamentous fungi, preventing alteration of morphology. (Poggeler and Kuck, 2004). During cell cycling, trafficking of various structures is a highly regulated process. Cell growth and the synthesis of additional genes needed to transition to subsequent cell cycle stages continues if specific genes are expressed at critical checkpoints. However, if genes that drive the cell cycle process are not expressed at the appropriate checkpoints, then cell cycle processes halt and programmed death

ensues. The absence of the WD gene, *Pro11*, by mutation suggests that the under-expression of regulatory genes may have prevented the fungal organism from reaching the next checkpoint required for maturation and alteration of its fruiting morphology. Similarly, *Hsp70* and WDRPUH may be required at appropriate checkpoints for *M. avidus* to transition through the stages of its cell cycle that includes transformation from microstome to the macrostome morphotpe. In this way, *Hsp70* and WDRPUH may be required to drive the transformation processes.

Additionally, two mRNA splicing genes, Step II splicing factor (*Slu7*) and a uridine-rich (subunit 1) small nuclear ribonucleoprotein-like U1 (snRNP) were isolated during microstome-to-macrostome transformation. *Slu7* genes have been isolated from yeasts, and more recently from human models. In the yeast and human models, *Slu7* is a housekeeping gene that activates the second step catalysis splicesome that separates introns from pre-messenger RNA (Chua and Reed, 2007; Umen and Gutherie, 1995; Zhou and Reed, 1998). *U1 snRNP*'s bind to pre-mRNA 5'end splice site and are held to this assembly by a zinc finger domain (Forch et al., 2002). Additionally, Zhou et al., (2002) demonstrated that some splicing genes are coupled to several steps downstream in gene expression, including transcription, polyadenylation, and mRNA export, although the distinct mechanisms are not completely understood (Zhou et al., 2002). The exact function of these genes in transforming *M. avidus* is unknown. It is clear that *Slu7* and *U1 snRNP* are up-regulated during mobilization of the transcription/translation machinery and may directly activate precursors required for transformation of the macrostome.

Lastly, a disulfide isomerase gene was isolated during transformation from microstome-to-macrostome. Disulfide isomerases have thioredoxin sulfide redox regions necessary for cleaving cysteine residues (Lundstrom and Holmgren, 1990). Four structurally distinct human disulfide isomerases were recently isolated from various stages of the life history of *Plasmodium falciparum* and are being assessed for future antimalarial agents (Mahaja et al., 2006). A disulfide isomerase localized in a chloroplast from *Chlamydomonas reinhardii* was identified as a reversible switch-regulating gene that controlled the activity between the chloroplast polyadenylate-binding proteins (Kim and Mayfield, 1997). In *M. avidus* disulfide isomerases may function as a reversible switch regulators that turns on genes that drive morphological alteration at the onset of microstome-to-macrostome transformation.

Genes Identified from *M. avidus* Tomite-to-Microstome Transformation

Cathepsin B and cathepsin L are members of the larger family of papain cysteine proteases. Cysteine proteases regulate protein degradation and turnover, hormone maturation, and enzyme activation in bacteria, plants, vertebrates and invertebrates (Berti et al., 1995; and Lecaille et al., 2002). Cathepsin B has been implicated in the progress of malignant diseases, acting in various ways to degrade the cell matrix and promote invasion of malignant cells during cancer metastasis (Nomura et al., 2004). Expression of cathepsin B increases invasive capabilities of many human carcinomas as well as certain protists through processes that are poorly

understood (Murnane et al., 1991; Nakae et al., 1998; Szpaderska and Frankfater, 2001).

Cathepsin B and other cysteine proteases have been isolated from *Plasmodium falciparum*, *Trypanosoma brucii*, and *Entamoeba histolytica* during developmental stages of their respective life histories (Bruchhaus et al., 2003; Hanspal et al., 2004; Mackey et al., 2004; Villalobo et al., 2003). Through mechanisms that are unclear, the parasites express cathepsin B at distinct stages of their respective histories in which the causative organism is invading its human hosts. For example, *Plasmodium falciparum* merozoites produce *Falcipain*-2, a cysteine protease required to invade host erythrocytes and feed on hemoglobin (Hanspal et al., 2004). Greenbaum et al., (2002) used a series of inhibition experiments (using *E64*, the same inhibitor used in this study) to prevent merozoites invasion. The non-parasitic ciliate, *Sterkiella histriomuscorum*, expresses cathepsin B and cathepsin L when transforming from a cyst to a feeding stage (Villalobo et al., 2003). In all instances, the expression of cathepsin B or other cysteine proteases in protistan organisms was coupled with transformation of the organism and subsequent feeding processes. While the specific function of *M. avidus* cathepsin B and L are unknown, their expression is also coupled with an alteration of overall cellular morphology that includes cell growth and synthesis of oral structures suitable for feeding on bacteria prey. Treating cells with *E64* and *Leupeptin* (two inhibitors of cysteine proteases) led to an arrest in the tomite-to-microstome transformation process at 2.5-hours (no further transformation occurred between 2.5 and 6-hours). The increased number of tomite-transformed-

microstomes between 0-2.5 hours in both treatments may have resulted from a lag-time required for the inhibitors to interact with their downstream substrates in the transformation mechanism. Thus, the inhibition experiments provided here, support the hypothesis that cysteine proteases coordinate the morphological changes of developing macrostome cortical and feeding structures.

In addition to cysteine proteases, potent cysteine protease inhibitors have also been isolated from a number of parasites during host invasion (Pandey et al., 2006; Scory et al., 2007). For example, *P. falciparum* merozoites expressed *falstatin*, an inhibitor of cysteine proteases during schizont rupture. Pandey et al., (2006) demonstrated that *falstatin* regulates many of its own cysteine proteases, including *falcipain*-2 and *falcipain*-3. Exposure to a cysteine protease inhibitor, diazomehtyl ketone inhibitor Z-Phe-Ala-CHN_2, caused *Trypanosoma cruzii* cells to transform from their typically long, slender shape to a "stumpy-like" more rounded form (Pandey et al., 2006). The inhibitor may have prevented cysteine proteases from interacting with genes that regulate the overall morphological architecture, resulting in aberrant cells. In addition to abnormal morphologies, the cysteine protease inhibitor prevented cell division in *T. cruzii* populations, thus altering some aspects of their cell cycle (Scory et al., 2007). Cell division does not occur once tomites are induced to become microstomes (Gomez-Saladin and Small 1993 b). Cysteine protease inhibitors may repress the expression of cell cycle genes that drive cell division, while promoting expression of genes that regulate other cellular functions. Similarly, expression of the

cysteine protease inhibitor, cystatin-1, may regulate tomite cell division, while promoting other genes that drive tomite-microstome transformation in *M. avidus*.

Several other genes of interest were isolated from the tomite-to-microstome transforming population. Ubiquitin Carboxyl-Terminal Hydrolase (UCH-L1) has numerous roles in the ubiquitin system important to regulating an array of biological activities, such as the proteolysis of ubiquinated proteins. For example, UCH-L1 mediated and enhanced neurogenesis in embryonic mice brains by regulating precursor embryonic cells (Sakurai et al., 2006). Additionally, increased expression of UCH-L1 caused high proliferation and migration renal cell carcinoma by suppressing apoptosis systems (Seliger et al., 2007). Ubiquitin has also been identified as a signaling component for many diverse cellular processes, such as the progression of cell cycle, DNA repair, and gene transcription (Kirkin et al., 2007). While an exact role has not been determined, UCH-1 apoptosis suppression may ensure that tomites persist long enough to find suitable feeding habitats during periods of starvation and may signal the synthesis of structures associated with cell growth and development of the oral apparatus.

Malate dehydrogenase, citrate synthase, and acetyl-coenzyme acyltransferase 1 are all enzymes associated with the citric acid cycle (Denton et al., 1975). Malate dehydrogenase converts malate into oxaloacetate so that it can be imported into the inner mitochondrial membrane. Citrate synthase catalyzes acetyl-coenzyme acyltransferase 1 and oxaloacetate, resulting in a six-carbon citrate, which continues

in the cycle eventually regenerating oxaloacetate (Voet 1995). The expression of these genes associated with metabolism was much higher in the tomite-to-microstome transforming populations and apparently under-expressed in the non-transforming microstomes. This was most likely because the tomites metabolic output accelerated upon return to feeding conditions.

Summary

Previous analyses of *Miamiensis avidus* provide a clear understanding of the morphological changes to the oral structures during life history transformation stages. However, the relationship between cell-signaling, signal interpretation and subsequent gene expression leading to the changes in the structure within polymorphic oligohymenophorean ciliates was unknown. This study examined gene expression of morphological transformations during two developmental stages of the polymorphic taxa, *M. avidus*. Using a suppression subtraction hybridization (SSH) procedure, a set of differentially expressed genes was identified for each transformation. Transformation from microstome-to-macrostome and from tomite-to-microstome included the expression of several genes integral to each process. The roles of two candidate genes, one from microstome-to-macrostome transformation (*Ef-1*α) and two from tomite-to-microstome, *M. avidus* transformations (cathepsin B and cathepsin L) were examined using a set of inhibition experiments. Inhibition successfully prevented the completion of their respective transformation processes. The role of two other genes from microstome-to-macrostome transformation (CCT transcription factor) and the tomite-to-microstome transformation (cystatin-1 cysteine protease inhibitor) were not assessed in this research. It is likely that more genes can be identified with additional rounds of SSH, refinement of the techniques provided here, and/or the use of other technologies such as microarray analysis. Genes identified from the two life history stages of *M. avidus* are ideal candidates for further studies and represent the first step of many, to understand the expression of genes

relative to alteration of structure within the polymorphic scuticociliates, and other Ciliophora.

References

Affa'a, F.M., Hickey, D.A., Struder-Kypke, M. & Lynn, D.H. 2004. Phylogenetic position of species in the genera *Anoplophrya*, *Plagiotoma*, and *Nyctheroides* (Phylum Ciliophora), endosymbiotic ciliates of annelids and anurans. *Journal of Eukaryotic Microbiology,* **51,** pp. 301-306.

Akaike, H. 1974. A new look at the statistical model identification. *IEEE Trans. Autom. Contr.,* **19,** pp. 716-723.

Berti, P.J. & Storer, A. C. 1995. Alignment/phylogeny of the papain superfamily of cysteine proteases. *Journal of Molecular Biology,* **246,** pp. 273-283.

Bradbury, P. 1989. Evidence for hymenostome affinities in an apostome ciliate. *Journal of Protozoology,* **36,** pp. 95-103.

Bradbury, P.C. 2005. *Gymnodinioides pitelkae* n. sp., (Ciliophora, Apostomatina) from the littoral amphipod, *Marinogammarus obtusatus*, a trophont with remnants of the tomite's infraciliature. *European Journal of Protistology,* **41,** pp. 85-92.

Bruchhaus, I., Loftus, B.J., Hall, N. & Tannich, E. 2003. The intestinal protozoan parasite *Entamoeba histolytica* contains 20 cysteine protease genes, of

which only a small subset is expressed during in vitro cultivation. *Eukaryotic Cell,* **2,** pp. 501-509.

Buchmann, K. & Nielsen, M. E. 1999. Chemoattraction of *Ichthyophthirius multifiliis* (Ciliophora) theronts to host molecules. *International Journal for Parasitology,* **29,** pp.1415-1423.

Buhse, H.E., Jr. 1967. Microstome-macrostome transformation in *Tetrahymena vorax* strain V2 type S induced by a transforming principle, stomatin. *The Journal of Protozoology,* **14,** pp. 608-613.

Butzel, H.M. & Fischer, J. 1983. The Effects of Purine and Pyrimidines Upon Transformation in *Tetrahymena-vorax* Strain V-2s. *Journal of Protozoology,* **30,** pp. 247-250.

Chomczynski, P. & Sacchi, N. 1987. Single-step method of RNA isolation by acid guanidinium thiocyanate-phenol-chloroform extraction. *Analytical Biochemistry,* **162,** pp. 156-159.

Chua, K. & Reed, R. 1999. Human step II splicing factor h*Slu7* functions in restructuring the spliceosome between the catalytic steps of splicing. *Genes & Development,* **13,** pp. 841-850.

Clamp, J.C. & Coats, D.W. 2000. *Planeticovorticella finleyi* n.g., n.sp. (Peritrichia, Vorticellidae), a planktonic ciliate with a polymorphic life cycle. *Invertebrate Biology,* **119,** pp. 1-16.

Corliss, J.O., 1956. On the evolution and systematics of cilated protozoa. *Systematic Zoology,* **5,** pp. 68-91.

Corliss, J.O., 1968. The value of ontogenetic data in reconstructing protozoan phylogenies. *Transactions of the American Microscopical Soceity,* **87,** pp. 1-20.

Corliss, J.O., 1972. *Tetrahymena* and some thoughts on the evolutionary origin of endoparasitism. *Transactions of the American Microscopical Society,* **91,** pp. 566-573.

Corliss, J.O., 1975. Taxonomic characterization of the suprafamilial groups in a revison of recently proposed schemes of classificaiton for the phylum Ciliophora. *Trans. Amer. Microsc. Soc.,* **94,** pp. 224-267.

Corliss, J.O., 1979. The ciliated protozoa: characterization, classification, and guide to the literature. Pergamon Press, Toronto.

Curry, A., & Butler, R.D 1982. Asexual reproduction in the suctorian *Discophrya collini*. *Protoplasma,* **111,** pp. 195-205.

Denton, R.M., Randle, P.J., Bridges, B.J., Cooper, R.H., Kerbey, A.L., Pask, H.T., Severson, D.L., Stansbie, D. & Whitehouse, S. 1975. Regulation of mammalian pyruvate dehydrogenase. *Mol Cell Biochem,* **9,** pp. 27-53.

Drummond, A.J., Kearse, M., Heled, J., Moir, R., Thierer, T., Ashton, B., Wilson, A. & Stones Havas, S. 2006. Geneious V.2.5. Available from http://www.geneious.com.

Egerter, D.E., Anderson, J.R. & Washburn, J.O. 1986. Dispersal of the parasitic ciliate *Lambornella clarki*: implications for ciliates in the biological control of mosquitoes. *Proceedings of the National Academy of Sciences of the United States of America,* **83,** pp.7335-7339.

Elwood, H.J., Olsen, G.J. & Sogin, M.L. 1985. The small-subunit ribosomal rna gene sequences from the hypotrichous ciliates *Oxytricha nova* and *Stylonychia pustulata*. *Molecular Biology and Evolution,* **2,** pp. 399-410.

Fauré-Fremiet, J., 1950. Morphologie compareé et systematique des ciliés. *Bullitin of the Society of Zoology, French,* **75,** pp. 109-122.

Felsenstein, J., 1981. Evolutionary trees from gene frequencies and quantitative characters finding maximum likelihood estimates. *Evolution,* **35,** pp. 1229 1242.

Fenchel, T., 1987. Ecological physiology: other aspects. In Ecology of Protozoa. pp. 63-68.

Foissner, W., 1993. Colpdea (Ciliophora). Gustav Fischer, Stuttgart, Germany.

Forch, P., Puig, O., Martinez, C., Seraphin, B. & Valcarcel, J. 2002. The splicing regulator TIA1 interacts with U1-C to promote *U1 snRNP* recruitment to 5' splice sites. *The EMBO Journal,* **21,** pp. 6882-6892.

Fox, D., Hill, B., & Chapman, G. 1992. Nuclear fine structure during development in *Heliophrya sp*., (Ciliophora: Suctoria). *Trans. Amer. Microsc. Soc.,* **111,** pp.128-142.

Gabe, P.R. & De Bault, L.E., 1973. Macromolecular syntheses related to the reproductive cyst of *Tetrahymena patula*. *J.Cell Biol.,* **59,** pp.615-623.

Gomez-Saladin, E. & Small, E.B. 1993a. Starvation induces tomitogenesis in *Miamiensis avidus* Strain Ma/2. *Journal of Eukaryotic Microbiology,* **40,** pp. 727-730.

Gomez-Saladin, E. & Small, E.B. 1993b. Oral morphogenesis of the microstome to macrostome transformation in *Miamiensis avidus* Strain Ma/2. *Journal of Eukaryotic Microbiology,* **40,** pp. 363-370.

Gomez-Saladin, E. & Small, E.B. 1993c. Prey-induced transformation of *Miamiensis avidus* Strain Ma/2 by a soluble factor. *Journal of Eukaryotic Microbiology,* **40,** pp. 550-556.

Grain, J. & De Puytorac, P. 1974. Ultrastructural particularities of kinetosomes and their fibrillar annexes in certain astomatous ciliates Hoplitophryidae. *Journal de Microscopie (Paris),***19,** pp. 231-246.

Grain, J., Senaud, J., de Puytorac, P., Zainab, B., & Jouany, J.P. 1979. Ciliate implantation in the rumen: influence of inoculated genus and type of diet. *Ann. Rech. Vet.,* **10,** pp. 264-267.

Greenbaum, D.C., Baruch, A., Grainger, M., Bozdech, Z., Medzihradszky, K.F., Engel, J., DeRisi, J., Holder, A.A. & Bogyo, M. 2002. A role for the protease *falcipain-1* in host cell invasion by the human malaria parasite. *Science,* **298,** pp. 2002-2006.

Grell, K.B. 1973. Protozoology. Springer-Verlag, New York, New York.

Griffiths, S., Dunford, R.P., Coupland, G. & Laurie, D.A. 2003. The evolution of CONSTANS like gene families in barley, rice, and *Arabidopsis*. *Plant Physiology,* **131,** pp. 1855-1867.

Gyrd-Hansen, M., Nylandsted, J. & Jaattela, M. 2004. Heat shock protein 70 promotes cancer cell viability by safeguarding lysosomal integrity. *Cell Cycle (Georgetown, Tex.),* **3,** pp.1484-1485.

Hammerschmidt, B., Schlegel, M., Lynn, D.H., Leipe, D.D., Sogin, M.L. & Raikov, I. B. 1996. Insights into the evolution of nuclear dualism in the ciliates revealed by phylogenetic analysis of rRNA sequences. *Journal of Eukaryotic Microbiology,* **43,** pp. 225-230.

Hanspal, M. 2000. cDNA cloning of a novel cysteine protease of *Plasmodium falciparum*. *Biochimica et Biophysica ACTA,* **1493,** pp. 242-245.

Hanspal, M., Dua, M., Takakuwa, Y., Chishti, A.H. & Mizuno, A. 2002. *Plasmodium falciparum* cysteine protease *falcipain-2* cleaves erythrocyte membrane skeletal proteins at late stages of parasite development. *Blood,* **100,** pp. 1048-1054.

Hausmann, K., and Bradbury, P.C., 1996. Ciliates: Cells as Organisms. Gustave Fischer, Stuttgart, Germany.

Hausmann, K., Hulsmann, N. & Radek, R. 2003. Protistology. Third edition**.** Berlin and Stuttgart, Germany.

Hoffman, G.L., Landolt, M., Camper, J.E., Coats, D.W., Stookey, J.L. & Burek, J. D. 1975. A disease of fresh water fishes caused by *Tetrahymena corlissi* and a key for identification of holotrich ciliates of fresh water fishes. *Journal of Parasitology,* **61,** pp. 217-223.

Hongiberg B.M., Bovee E.C., Corliss J.O., Gojdics M., Hall R.P., Kudo R.R., Levine N.D., Loeblich A.R., Weiser J., & Wenrich D.H. 1964. A revised classification of the phylum Protozoa. *Journal of Protozoology,* **11,** pp. 7-20.

Huelsenbeck, J.P. & Ronquist, F. 2001. MRBAYES: Bayesian inference of phylogenetic trees. *Bioinformatics (Oxford),* **17,** pp. 754-755.

Jankowski, A.W. 1972. Recaptulation of phylogenesis in ciliate ontogeny. In: Vorontsov NN(ed.) Problems of evolution. *Akad Nauk SSSR,* Vol. 2**:** Nauka, Novosibrsk, pp. 95-123 (in Russian with English summary).

Jankowski, A.W. 1985. Life cycles and taxonomy of generic groups Scyphidia, Heteropolaria, Zoothamnium and Cothurnia (class Peritricha). *Trudy Zool Inst., Lenningrad,* **129,** pp 74 100 (in Russian).

Jung, S.J., Kitamura, S., Song, J.Y. & Oh, M.J. 2007. *Miamiensis avidus* (Ciliophora: Scuticociliatida) causes systemic infection of olive flounder *Paralichthys olivaceus* and is a senior synonym of *Philasterides dicentrarchi*. *Diseases of Aquatic Organisms,* **73,** pp. 227-234.

Keenan, R.W., and Holloman, L. 1973. Studies on the biosynthesis of glucolipid in *Tetrahymena pyriformis*. *Biochim. Biophys. Acta,* **326,** pp. 84-92.

Kim, J. & Mayfield, S.P. 1997. Protein disulfide isomerase as a regulator of chloroplast translational activation. *Science (New York, N.Y.),* **278,** pp. 1954 1957.

Kirkin, V. & Dikic, I. 2007. Role of ubiquitin- and Ubl-binding proteins in cell signaling. *Current Opinion in Cell Biology,* **19,** pp. 199-205.

Kopp, M. & Tollrian, R. 2003. Trophic size polyphenism in *Lembadion bullinum*: costs and benefits of an inducible offense. *Ecology,* **84,** pp. 641-651.

Landers, S.C., Gomez-Gutierrez, J. & Peterson, W.T. 2006. *Gymnodinioides pacifica*, n. sp., an exuviotrophic ciliated protozoan (Ciliophora, Apostomatida) from euphausiids of the Northeastern Pacific. *European Journal of Protistology,* **42,** pp. 97-106.

Lecaille, F., Kaleta, J. & Bromme, D. 2002. Human and parasitic *papain*-like cysteine proteases: their role in physiology and pathology and recent developments in inhibitor design. *Chemical Reviews,* **102,** pp. 4459-4488.

Lennartz, D. C. & Bovee, E. C. 1980. Induction of macrostome formation in *Blepharisma americanum* (Suzuki, 1954) by alpha-tocopheryl succinate. *Transactions of the American Microscopical Society,* **99,** pp. 312-317.

Lim, S.U., Seo, J.S., Kim, M.S., Ahn, S.J., Jeong, H.D., Kim, K.H., Park, N.G., Kim, J.K., Chung, J.K. & Lee, H.H. 2005. Molecular cloning and characterization of Cathepsin Bfrom a scuticociliate, *Uronema marinum*. *Comparative Biochemistry and Physiology Part B, Biochemistry & Molecular Biology,* **142,** pp. 283-292.

Lom, J., Corliss, J.O. & Noirot-Timothee, C. 1968. Observations on the ultrastructure of the buccal apparatus in thigmotrich ciliates and their bearing on thigmotrich peritrich affinities. *The Journal of Protozoology,* **15,** pp. 824-840.

Lundstrom, J. & Holmgren, A. 1990. Protein disulfide-isomerase is a substrate for thioredoxin reductase and has thioredoxin-like activity. *Journal Biol. Chem.,* **265,** pp. 9114-9120.

Lynn, D.H., & Small, E.B. 2000. Phylum Ciliophora. In: Lee, J. J., Hutner, S. H., & Bovee, E. C. (ed.): An Illustrated Guide to the Protozoa. 2nd edition, Society of Protozoologists Special Publication, Allen Press, Lawrence, Kansas.

Lynn, D.H. & Struder-Kypke, M. 2004. Phylogenetic relationships among species in the genera *Entodiscus*, *Plagiophyliella*, *Thyrophylax*, and *Entorhipidium*, scuticociliate endosymbionts of echinoids. *Journal of Eukaryotic Microbiology,* **51,** pp. 5A-6A.

Mackey, Z.B., O'Brien, T.C., Greenbaum, D.C., Blank, R.B. & McKerrow, J.H. 2004. A cathepsin B-like protease is required for host protein degradation in *Trypanosoma brucei. Journal of Biological Chemistry,* **279,** pp. 48426-48433.

Maddison, W.P. & Maddison, D.R. 1989. Interactive Analysis of Phylogeny and Character Evolution Using the Computer Program MacClade. *Folia Primatologica,* **53,** pp. 190-202.

Mahajan, B., Noiva, R., Yadava, A., Zheng, H., Majam, V., Krishna Mohan, K.V., Moch, J.K., Haynes, J.D., Nakhasi, H. & Kumar, S. 2006. Protein disulfide

isomerase assisted protein folding in Malaria parasites. *International Journal for Parasitology,* **36,** pp. 1037-1048.

Malave, T. M. & Forney, J. D. 2004. Identification of a developmentally regulated translation elongation factor 2 in *Tetrahymena thermophila*. *Gene (Amsterdam),* **326,** pp. 97-105.

McArdle, E. W., Bergquist, B.L. & Ehret, C.F. 1980. Structural changes in *Tetrahymena rostrata* during induced encystment. *Journal of Protozoology,* **27,** pp. 388-397.

McKay, D. B. 1993. Structure and mechanism of 70-kDa heat-shock-related proteins. *Advances in Protein Chemistry,* **44,** pp. 67-98.

Medlin, L., Elwood, H.J., Stickel, S. & Sogin, M.L. 1988. The characterization of enzymatically amplified eukaryotic 16s-like ribosomal rna-coding regions. *Gene (Amsterdam),* **71,** pp. 491-500.

Messick, G.A. & Small, E.B. 1996. *Mesanophrys chesapeakensis* n. sp., a histophagous ciliate inthe blue crab, *Callinectes sapidus*, and associated histopathology. *Invertebrate Biology,***115,** pp. 1-12.

Miao, W., Fen, W. S., Yu, Y. H., Zhang, X. Y. & Shen, Y. F. 2004. Phylogenetic relationships of the subclass Peritrichia (Oligohymenophorea, Ciliophora) inferred from small subunit rRNA gene sequences. *The Journal of Eukaryotic Microbiology,* **51,** pp. 180-186.

Moewus, L. 1962. Studies on a marine parasitic *Tetrahymena* species. *Journal of Protozoology,* **9 (Suppl.),** p. 13.

Mohr, J.L., Matsudo, H., & Leung, Y.M. 1970. The ciliate taxon Chonotricha. *Oceanogr. Mar. Biol. Anuu. Rev.,* **8,** pp. 415-456.

Montagnes, D.J., & Lynn, D.H., 1987. A quantitative protargol stain (QPS) for ciliates: a method description and test of its quantitative nature. *Mar. Microb. Food Webs,* **2,** pp. 83-93.

Montagnes, D.J., & Lynn, D.H., 1993. A quantitative protargol stain (QPS) for ciliates and other protists. In Kemp, P.F., et al. (eds.) Handbook of Methods in Aquatic Microbial Ecology. Lewis Publisher, Boca Raton, pp. 229-240.

Munday, B.L., O'Donoghue, P.J., Watts, M., Rough, K. & Hawkesford, T. 1997. Fatal encephalitis due to the scuticociliate Uronema *nigricans* in sea-caged, southern bluefin tuna *Thunnus maccoyii*. *Diseases of Aquatic Organisms,* **30,** pp. 17-25.

Murnane, M.J., Sheahan, K., Ozdemirli, M. & Shuja, S. 1991. Stage-specific increases in cathepsin B messenger RNA content in human colorectal carcinoma. *Cancer Research,* **51,** pp. 1137-1142.

Nakae, T., Horai, T., Imamura, F., Akedo, H. & Higashino, K. 1998. Expression of cathepsin B in small cell lung carcinoma cells in relation to in vitro invasiveness. *Tumor Biology,* **19,** pp. 118-125.

Nanney, D.L., & McCoy, J.W. 1976. Characterization of the species of *Tetrahymena pyriformis* complex. *Journal of Amer. Microsc. Soc.,* **45,** pp.1335-1358.

Neer, E.J., Schmidt, C.J., Nambudripad, R. & Smith, T.F. 1994. The ancient regulatory-protein family of WD-repeat proteins. *Nature,* **371,** pp. 297-300.

Nijine, T. 1972. La transformation microstome-macrostome et macrostome-microstome chez *Tetrahymena paravorax*. *Annals de la Faculté des Sciences du Cameroun,* **10,** pp. 69-84.

Nomura, T., 2005. Involvement of cathepsins in the invasion, metastasis, and proliferation of cancer cells. *Journal of Medical Investigation* **34,** pp. 1-9.

Nylander, J.A., Ronquist, F., Huelsenbeck, J.P. & Nieves-Aldrey, J.L. 2004. Bayesian phylogenetic analysis of combined data. *Systematic Biology,* **53,** pp. 47-67.

Nylandsted, J., Gyrd-Hansen, M., Danielewicz, A., Fehrenbacher, N., Lademann, U., Hoyer Hansen, M., Weber, E., Multhoff, G., Rohde, M. & Jaattela, M. 2004. Heat shock protein 70 promotes cell survival by inhibiting lysosomal membrane permeabilization. *The Journal of Experimental Medicine,* **200,** pp. 425-435.

Pandey, K.C., Singh, N., Arastu-Kapur, S., Bogyo, M. & Rosenthal, P.J. 2006. *Falstatin*, a cysteine protease inhibitor of *Plasmodium falciparum*, facilitates erythrocyte invasion. *PLoS Pathogens,* **2,** p. 117.

Parama, A., Iglesias, R., Alvarez, F., Leiro, J.M., Quintela, J.M., Peinador, C., Gonzalez, L., Riguera, R. & Sanmartin, M.L. 2004. In vitro efficacy of new antiprotozoals against *Philasterides dicentrarchi* (Ciliophora, Scuticociliatida). *Diseases of Aquatic Organisms,* **62,** pp. 97-102.

Perez-Uz, B. & Guinea, A. 2001. Morphology and infraciliature of a marine scuticociliate with a polymorphic life cycle: *Urocryptum tortum* n. gen., n. comb. *Journal of Eukaryotic Microbiology,* **48,** pp. 338-347.

Poggeler, S. & Kuck, U. 2004. A WD40 repeat protein regulates fungal cell differentiation and can be replaced functionally by the mammalian homologue *striatin*. *Eukaryotic cell,* **3,** pp. 232-240.

Posada, D. & Crandall, K.A. 1998. MODELTEST: Testing the model of DNA substitution. *Bioinformatics (Oxford),* **14,** pp. 817-818.

Puytorac, P. d., Grain, J., & Mignot, J.P., 1987. Precis de Protistologie. Boubee, Paris, pp. 112-120.

Puytorac, P. d., Batisse, A., Bohatier; J., Corliss, J.O., Deroux, G., Didier, P., Dragesco, J., Fryd-Versavel, G., Grain, J., Grolière, C.A., Hovasse, R., Iftode, F., Laval, M., Rogue, M., Savoie, A., & Tuffrau, M.. 1974. Proposition d'une classification du phylum Ciliophora Doflein, 1901. *Comptes Rendus de l'Académie de Sciences,* **278,** pp. 2799-2802.

Ragan, M. A., Cawthorn, R.J., Despres, B., Murphy, C.A., Singh, R.K., Loughlin, M.B. & Bayer, R.C. 1996. The lobster parasite *Anophryoides haemophilia* (Scuticociliatida: Orchitophyridae): nuclear 18S rDNA sequence, phylogeny and detection using oligonucleotide primers. *Journal of Eukaryotic Microbiology,* **43,** pp. 341-346.

Ramsey, J.M., 1981. The Biology of *Potomacus pottsi* (Scuticociliatida, Ciliophora). Aspects of fine structure, osmoregulation, polymorphism, and systematics. *Ph.D Dissertation. Georgetown University, Washington DC*.

Ramsey, J.M., Brownlee, D. C. & Small, E. B. 1980. *Potomacus pottsi* Thompson 1967 (Scuticociliatida, Ciliophora): stomatogenesis with redescription of the microstome trophont. *Transactions of the American Microscopical Society,* **99,** pp. 43-51.

Ravagnan, L., Gurbuxani, S., Susin, S.A., Maisse, C., Daugas, E., Zamzami, N., Mak, T., Jaattela, M., Penninger, J. M., Garrido, C. & Kroemer, G. 2001. Heat-shock protein 70 antagonizes apoptosis-inducing factor. *Nature Cell Biology,* **3,** pp. 839-843.

Rawlinson, N.G. & Gates, M.A. 1986. A morphological classification of encysting species of euplotes (Ciliophora: Nassophorea: Euplotida). *Transactions of the American Microscopical Soceity,* **105,** pp. 301-310.

Rebrikov, D.V., Britanova, O.V., Gurskaya, N.G., Lukyanov, K.A., Tarabykin, V.S. & Lukyanov, S.A. 2000. Mirror orientation selection (MOS): a method for eliminating false positive clones from libraries generated by suppression subtractive hybridization. *Nucleic Acids Research,* **28,** p. E90.

Rhode, M., Daugaard, M., Jensen, M.H., Helin, K., Nylandsted, J. & Jaattela, M. 2005. Members of the heat-shock protein 70 family promote cancer cell growth by distinct mechanisms. *Genes & Development,* **19:**570-582.

Ricci, N., Grandini, G., Bravi, A. & Banchetti, R. 1991. The giant of Oxytricha bifaria, a peculiar cell differentiation triggered and controlled by cell-to-cell contacts. *European Journal of Protistology,* **27,** pp. 127-133.

Ronquist, F. & Huelsenbeck, J.P. 2003. MrBayes 3: Bayesian phylogenetic inference under mixed models. *Bioinformatics (Oxford),* **19,** pp. 1572-1574.

Ryals, P.E., Bae, S. & Patterson, C.E. 1999. Evidence for early signaling events in stomatin induced differentiation of *Tetrahymena vorax*. *Journal of Eukaryotic Microbiology,* **46,** pp. 77-83.

Sakurai, M., Ayukawa, K., Setsuie, R., Nishikawa, K., Hara, Y., Ohashi, H., Nishimoto, M., Abe, T., Kudo, Y., Sekiguchi, M., Sato, Y., Aoki, S., Noda, M. & Wada, K. 2006. Ubiquitin C-terminal hydrolase L1 regulates the morphology of neural progenitor cells and modulates their differentiation. *Journal of Cell Science,* **119,** pp. 162-171.

Savoie, A. 1962. *Ophryoglena faurei* n. sp. (Ciliata, Hymenostomatida, Ophryoglenidae) reproduction cycles. *The Journal of Protozoology,* **9,** pp. 427-434.

Schmidt, S.L. & Schlegel, M., Bernhard, D., 2007. Molecular phylogeny of the Heterotrichea (Ciliophora, Postciliodesmatophora) based on small subunit rRNA gene sequences. *J. of Eukaryotic Microbiology,* **54,** pp. 358-363.

Schwarz, G. 1974. Estimating the dimension of a model. *Ann. Stat.,* **6,** pp. 461-464.

Scory, S., Stierhof, Y.D., Caffrey, C.R. & Steverding, D. 2007. The cysteine proteinase inhibitor Z-Phe-Ala-CHN2 alters cell morphology and cell division activity of *Trypanosoma brucei* bloodstream forms in vivo. *Kinetoplastid Biology and Disease,* **6,** pp. 201-212.

Seliger, B., Lichtenfels, R., Handke, D., Fedorushchenko, A., Brenner, W., Yi, F., Dammann, R., Atkins, D., Ferrone, S. & Hanash, S. 2006. Ubiquitin carboxylterminal hydrolase-1: A biomarker of renal cell carcinoma and melanoma. *Proceedings of the American Association for Cancer Research Annual Meeting,* **47,** pp. 331-342.

Shiina, N., Gotoh, Y., Jubomura, N., Iwamatsu, A. & Nishida, E. 1994. Microtubule severing by Elongation Factor 1. *Science,* **266,** pp. 282-285.

Shu, D.G., Conway Morris, S., Han, J., Zhang, Z.F., Yasui, K., Janvier, P., Chen, L., Zhang, X.L., Liu, J. N., Li, Y. & Liu, H.Q. 2003. Head and backbone of the Early Cambrian Haikouichthys. *Nature,* **421,** pp. 426-429.

Silva, F. P., Hamamoto, R., Nakamura, Y. & Furukawa, Y. 2005. WDRPUH, a novel WD repeat-containing protein, is highly expressed in human hepatocellular carcinoma and involved in cell proliferation. *Neoplasia (New York, N.Y.),* **7,** pp. 348-355.

Small, E.B. 1967. The Scuticociliatida, a new order of the Class Ciliatea (Phylum Protozoa, Subphylum Ciliophora). *Transactions of the American Microscopical Society,* **86,** pp.345-370.

Small, E.B., & Lynn, D.H. 1985. Phylum Ciliophora. In: Lee, J. J., Hutner, S. H., & Bovee, E. C. (ed.): An Illustrated Guide to the Protozoa**,** 1st Ed**.** Society of Protozoologists Special Publication, Allen Press, Lawrence, Kansas.

Small, E.B., Heisler, J., Sniezek, J. & Illife, T. 1986. *Glauconema bermudense* n. sp. (Scuticociliatida, Oligohymenophorea), a troglobitic ciliophorean from Bermudian marine caves. *Stylogia,* **2,** pp. 167-179.

Snoeyenbos-West, O., Cole, J., Campbell, A., Coats, D.W., & Katz, L. 2004. Molecular phylogeny of phyllopharyngean ciliates and their group I introns. *Journal of Eukaryotic Microbiology,* **51,** pp. 441-450.

Sogin, M.L., Karlok, M., Nielsen, H., & Engberg, J., 1986. Phylogenetic evidence for the acquisition of ribosomal RNA introns subsequent to the divergence of some of the major *Tetrahymena groups*. *EMBO J.,* **5,** pp. 3625-3630.

Soldo, A.T. & Merlin, E. 1971. The Cultivation of Marine Ciliates in Axenic Medium. *Journal of Protozoology,* **18,** pp. 12-23.

Spangler, E.A. 1985. The nucleotide sequence of the 17S ribosomal RNA gene of *Tetrahymena thermophila* and the identification of point mutations resulting in resistance to the antibiotics paromomycin and hygromycin. *J. Biol. Chem.,* **260,** pp. 6334-6340.

Stechmann, A.M, & Lynn, D.H. 1998. Phylogenetic relationships between prostome and colpodean ciliates tested by small subunit rRNA. *Mol. Phylogenet. Evol.,* **9,** pp. 48-54.

Stone, G.E., & Cmeron, I.L. 1964. Methods for using *Tetrahymena* in studies of the normal cell cycle. In: Methods in Cell Physiology, Vol. 1 Prescott, D.M. (ed.). New York and London: Academic Press**,** pp. 127-140.

Strayer, C., Oyama, T., Schultz, T.F., Raman, R., Somers, D.E., Mas, P., Panda, S., Kreps, J.A. & Kay, S.A. 2000. Cloning of the *Arabidopsis* clock gene TOC1, an autoregulatory response regulator homolog. *Science (New York, N.Y.),* **289,** pp. 768-771.

Struder-Kypke, M.C., Wright, A.D., Fokin, S.I., & Lynn, D.H., 2000. Phylogenetic relationships of the Subclass Peniculia (Oligohymenophorea, Ciliophora) inferred from small subunit rRNA gene sequences. *Journal of Eukaryotic Microbiology,* **47,** pp. 419-429.

Struder-Kypke, M.C., Wright, A.D., Jerome, C.A. & Lynn, D.H., 2001. Parallel evolution of histophagy in ciliates of the genus *Tetrahymena*. *BMC Evolutionary Biology,* **1,** pp. 1-9.

Swofford, D.L. 2002. PAUP* Phylogenetic Analysis Using Parsimony (and Other Methods). Version 4. Sinauer Associates, Sunderland, Massachusetts.

Szpaderska, A.M. & Frankfater, A. 2001. An intracellular form of cathepsin B contributes to invasiveness in cancer. *Cancer Research,* **61,** pp. 3493-500.

Thompson, J.C., Jr. 1966. *Potomacus pottsi* n.g., n. sp., a hymenostome ciliate from the Potomac River. *Journal of Protozoology,* **13,** pp. 393-395.

Thompson, J.C., Jr. & Moewus, L. 1964. *Miamiensis avidus* n. g., n. sp., a marine facultative parasiste in the ciliate order Hymenostomatida. *Journal of Protozoology,* **11,** pp. 378-381.

Thompson, J.D., Gibson, T.J., Plewniak, F., Jeanmougin, F. & Higgins, D.G. 1997. The CLUSTAL-X windows interface: Flexible strategies for multiple sequence alignment aided by quality analysis tools. *Nucleic Acids Research,* **25,** pp. 4876-4882.

Tokumoto, T., Kondo, A., Miwa, J., Horiguchi, R., Tokumoto, M., Nagahama, Y., Okida, N. & Ishikawa, K. 2003. Regulated interaction between polypeptide chain elongation factor-1 complex with the 26S proteasome during Xenopus oocyte maturation. *BMC Biochemistry,* **4,** pp. 6-15.

Tokuyasu, K. & Scherbaum, O.H. 1965. Ultrastructure of mucocysts and pellicle of *Tetrahymena pyriformis*. *Journal Cell Biology,* **27,** pp. 67-81.

Tuhackova, Z., Ullrichova, J. & Hradec, J. 1985. Regulation of the activity of eukaryotic peptide elongation factor 1 by autocatalytic phosphorylation. *European Journal of Biochemistry / FEBS,* **146,** pp. 161-166.

Umen, J.G. & Gutherie, C. 1995. The second catalytic step of pre-mRNA splicing. *RNA,* **1,** pp. 869-885.

Utz, L.R., & Eizirik, E., 2007. Molecular phylogenetics of the subclass Peritrichia (Ciliophora: Oligohymenophorea) based on expanded analyses of 18S rRNA sequences. *Journal of Eukaryotic Microbiology,* **54,** pp. 303-305.

Viljoen, S., & Van As, J.G. 1987. Notes on morphology and asexual reproduction processes of sessile peritrichs. *Hydrobiologia,* **154,** pp. 75-86.

Villalobo, E., Moch, C., Fryd-Versavel, G., Fleury-Aubusson, A. & Morin, L. 2003. cysteine proteases and cell differentiation: excystment of the ciliated protist *Sterkiella histriomuscorum*. *Eukaryotic Cell,* **2,** pp. 1234-1245.

Voet, D. & Voet, J. 1995. Biochemistry, 2nd Edition. John Wiley & Sons, New York.

Wang, X., Campbell, L., Miller, C. & Pourd, C. 1998. Amino acid availability regulates p70 S6 kinase and multiple translation factors. *Biochem. J.,* **334,** pp. 261-267.

Washburn, J.O., Gross, M.E., Mercer, D.R. & Anderson, J.R. 1988. Predator-induced trophic shift of a free-living ciliate: parasitism of mosquito larvae by their prey. *Science (New York, N.Y.),* **240,** pp. 1193-1195.

Wicklow, B. 1988. Developmental polymorphism induced by intraspecific predation in the ciliated protozoan, *Onchodromus quadricornutus*. *Journal of Protozoology,* **35,** pp. 137-141.

Williams, N. 1960. The polymorphic life history of *Tetrahymena patula*. *Journal of Protozoology,* **7,** pp. 10-17.

Williams, N.E., Honts, J. E. & Dress, V.M. 1992. Protein polymorphism and evolution in the genus *Tetrahymena*. *Journal of Protozoology,* **39,** pp. 54-58.

Wright, A.D., Dehority, B.A. & Lynn, D.H. 1997. Phylogeny of the rumen ciliates *Entodinium*, *Epidinium* and *Polyplastron* (Litostomatea:Entodiniomorphida) inferred from small subunit ribosomal RNA sequences. *Journal of Eukaryotic Microbiology,* **44,** pp. 61-67.

Zhang, X.L., Han, J., Zhang, Z.F., Liu, H.Q. & Shu, D.G. 2003. Reconsideration of the supposed naraoiid larva from the early Cambrian Chengjiang Lagerstatte, South China. *Palaeontology (Oxford),* **46,** pp. 447-465.

Zhou, Z., Licklider, L.J., Gygi, S.P. & Reed, R. 2002. Comprehensive proteomic analysis of the human spliceosome. *Nature,* **419,** pp. 182-185.

Zhou, Z. & Reed, R. 1998. Human homologs of yeast prp16 and prp17 reveal conservation of the mechanism for catalytic step II of pre-mRNA splicing. *The EMBO Journal,* **17,** pp. 2095-2106.

Zwickl, D. J. 2006. Gentic algorithm approaches for the phylogenetic analysis of large biological sequence datasets under the maximum likelihood criterion. Ph.D. Dissertation, Univeristy of Texas at Austin.